Aus der Klinik für Allgemein-, Viszeral- und Kinderchirurgie
der Heinrich-Heine-Universität Düsseldorf
Direktor: Univ.-Prof. Dr. med. Wolfram T. Knoefel

Two magnetic enrichment methods for pancreatic circulating tumour cells detection

Dissertation

zur Erlangung des Grades eines Doktors der Medizin der Medzinischen Fakultät der Heinrich-Heine-Universität Düsseldorf

vorgelegt von

Junhao Wu

2023

Als Inauguraldissertation gedruckt mit der Genehmigung der
Medizinischen Fakultät der Heinrich-Heine-Universität Düsseldorf

gez.:
Dekan: Prof. Dr. med. Nikolaj Klöcker
Erstgutachter: Prof. Dr. med. Stoecklein
Zweitgutachter: Prof. Dr. rer. nat. Neubauer

Teile dieser Arbeit wurden veröffentlicht:

MAGNETIC-BASED ENRICHMENT OF RARE CELLS FROM HIGH CONCENTRATED BLOOD SAMPLES, Junhao Wu, Katharina Raba, Rosa Guglelmi, Bianca Behrens, Guus Van Dalum, Georg Flügen, Andreas Koch, Suraj Patel, Wolfram T. Knoefel, Nikolas H. Stoecklein And Rui P. L. Neves, CANCERS 2020, 12(4), 933

ZUSAMMENFASSUNG

In den letzten Jahrzehnten gab es bedeutende technische Entwicklungen auf dem Gebiet der Flüssigbiopsien, die unseren Zugang zu zirkulierenden Tumorzellen (CTCs) verbessert haben. Bei einigen Tumorarten, wie dem duktalen Adenokarzinom des Pankreas, sind die Erkennungsrate und die Anzahl der nachgewiesenen CTCs jedoch immer noch sehr niedrig, was die Verwendung von CTCs als Biomarker und Tumorgewebeersatz für die molekulare Analyse beeinträchtigt. Eine Haupteinschränkung besteht in dem geringen Blutvolumen, das in Standard-CTC-Assays gescreent wird. Die diagnostische Leukapherese ermöglicht die Entnahme literweise Blut und stellt eine vielversprechende alternative Strategie dar, um eine größere Anzahl von CTCs zu sammeln, jedoch stellt die hohe zelluläre Konzentration dieser Produkte eine zusätzliche Herausforderung für die CTC-Anreicherung mit den bestehenden CTC-Assays dar. In der vorliegenden Arbeit habe ich die technische Leistungsfähigkeit von zwei Systemen zur Anreicherung und Detektion seltener Tumorzellen in hochkonzentrierten Blutprodukten untersucht: dem Isoflux und dem KingFisher. Das erste ist speziell für CTC-Anreicherungszwecke im Handel erhältlich, während das zweite System das Design und die Optimierung von Protokollen für diese Anwendung erforderte. Beide Methoden basieren auf der immunomagnetischen Anreicherung, und ich habe die Leistung unter Verwendung verschiedener Arten von magnetischen Kügelchen und unter Verwendung von EpCAM und MUC-1 als Epitope getestet, die auf die Oberfläche der Tumorzellen gerichtet sind. Obwohl die Anreicherung seltener Zellen mit beiden Systemen möglich war, war die Leistung von KingFisher in der jeweiligen experimentellen Umgebung überlegen. Darüber hinaus konnte ich im KingFisher die Anreicherung und die anschließende Immunfärbung in einem einzigen automatisierten Protokoll vereinen, wodurch die erforderliche praktische Zeit reduziert wurde. Zudem konnte ich im KingFisher-System Protokolle erstellen, in denen verschiedene Beads für die Depletion hämatogener Zellen vor der positiven Selektion von CTCs kombiniert wurden. Dieses Werk zeigt insgesamt die hohe Flexibilität in Bezug auf magnetische Perlen und die hohe Kosteneffektivität. Es zeigt auch die Möglichkeit, die Färbung zu automatisieren und den Eingriff des Bedieners zu reduzieren, sowie die Möglichkeit, eine große Anzahl von Proben parallel im KingFisher-System zu verarbeiten. Die gesammelten Ergebnisse legen nahe, dass dies eine attraktive Lösung zur Verarbeitung großer Blutvolumina darstellen könnte.

SUMMARY

In the last decades there has been significant technical developments in the field of liquid biopsies that have improved our access to circulating tumour cells (CTCs). However, for some tumour types, as the pancreatic ductal adenocarcinoma, the detection rate and number of CTCs detected are still very low which compromises the use of CTCs as biomarker and tumour tissue surrogate for molecular analysis. A major limitation resides on the low volume of blood that is screened in standard CTC assays. Diagnostic leukaphaeresis allow to sample liters of blood and constitutes a promising alternative strategy to collect higher numbers of CTCs, however the high cellular concentration of these products constitutes additional challenging for CTC enrichment with the existing CTC assays. In the present work I explored the technical performance of two systems for enrichment and detection of rare tumour cells in highly concentrated blood products: The Isoflux and the KingFisher. The first is commercially available specifically for CTC enrichment purposes, while the second system required the design and optimization of protocols for this application. Both methods are based in immunomagnetic enrichment and I tested the performance using several types of magnetic beads and using EpCAM and MUC-1 as epitopes targeted at surface of the tumour cells. Despite enrichment of rare cells was possible with both systems, in the particular experimental setting, the performance of KingFisher was superior. Furthermore, in the KingFisher I could unify enrichment and subsequent immunostaining in a single automated protocol reducing the hands-on time necessary. Additionally, in the KingFisher system, I could establish more complex protocols combining different beads for initial depletion of hematogenous cells prior positive selection of CTCs. This work demonstrates the high flexibility in terms of magnetic beads and the high cost-effectiveness. It also shows the possibility to automate staining and reduce the operator intervention, and the possibility to parallel process a high number of samples in the KingFisher system. The results collected suggest that it might constitute an attractive solution to process large blood volumes.

List of abbreviation

CA 19-9	Carbohydrate-Antigen 19-9
CEA	Carcinoembryonic Antigen
CK	Cytokeratin
CT	Computed Tomography
CTC	Circulating Tumour Cells
DAPI	4´6-Diamidino-2-Phenylindole
DEP	Dielectrophoresis
DLA	Diagnostic Leukapheresis
Dy-BioB	Dynabeads™ Biotin Binder
Dy-EpE	Dynabeads™ Epithelial Enrich
EpCAM	Epithelial Cell Adhesion Molecule
EMT	Epithelial-Mesenchymal Transition
FACS	Fluorescence-Activated Cell Sorting
ISO-CEK	IsoFlux CTC Enrichment Kit
ISO-RCEK	IsoFlux Rare Cell Enrichment Kit
MNCs	Mononuclear Cells
MRI	Magnetic Resonance Imaging
NET	Neuroendocrine Tumour
OS	Overall Survival
PBMCs	Peripheral Blood Mononuclear Cells
PDAC	Pancreatic Ductal Adenocarcinoma
VNTR	Variable Number Tandem Repeat

Table of contents

1 – INTRODUCTION

1.1 – Pancreatic cancer and circulating tumour cells (CTCs)

Cancer of the pancreas is one of the cancers with worst prognosis. It resulted in 411,600 deaths globally in 2015 and is one of the most common causes of cancer death [1], especially in patients with metastasis. The 1-year survival rate ranges from 17-23%, and the 5-year survival rate is less than 5% [1,2]. Even with recent advances in multimodal therapies including modern surgical techniques, the overall survival (OS) of pancreatic cancer has only increased slightly [3]. Early diagnosis is crucial for improving pancreatic cancer prognosis. However, this has been hindered by the relatively low specificity and sensitivity of blood biochemical tests (such as the tests for carbohydrate-antigen 19-9 (CA 19-9) and carcinoembryonic antigen (CEA)), or of expensive imaging examinations (such as computed tomography (CT) scans or magnetic resonance imaging (MRI)) [4]. Furthermore, the anatomy of the organ limits options for biopsies, which are technically quite challenging.

Circulating tumour cells (CTCs) are becoming a focus point of cancer research [5]. This type of tumour cell originates from solid tumours, can survive in the circulatory system, and can proliferate in a suitable environment, leading to tumour recurrence and metastasis. The mechanisms by which CTCs leave the primary tumour are still under investigation and have not been fully unraveled. For example, a matter of substantial debate is the role of the epithelial-mesenchymal transition (EMT) in the origin and also in the phenotype of CTCs. In addition, it is still unclear why not every CTC has the ability to establish metastasis and what might be the genetic, epigenetic and/or environmental factors determining higher metastatic competence of particular CTCs [6]. However, CTC analysis has been verified to provide useful information for risk classification, evaluation of treatment efficacy, and early detection of cancer recurrence [7,8]. In pancreatic cancer, the number of CTCs in a patient associates with the chance of metastasis or the stage of the disease [9,10]. Some studies showed that CTC-positive patients had shorter survival and poorer prognosis even after surgical resection [11,12]. Further, the number of CTCs also reflects the clinical response to chemotherapy [13]. In addition to their value as biomarkers, CTCs can provide insights into the biology and molecular profile of the

respective tumour, the mechanisms of cancer progression, relevant biomarkers for cancer detection and treatment, and the molecular pathways active in cancer metastasis.

1.2 – CTC detection

1.2.1 – Principles of pancreatic CTC enrichment and detection

Compared with the large number of blood cells in blood samples, the number of CTCs in the blood can be considered negligible. Typically, 1-10 CTCs can be found in per mL of whole blood in less than 50% of metastatic patients [14]. The accurate separation of CTCs from the abundant background of hematogenous cells in a blood sample remains a difficult challenge. To deal with this problem, a significant number of platforms for CTC enrichment and enumeration have been developed. These technologies follow one of two strategies: One is immunoaffinity based on cell surface molecular markers (marker dependent), which use either tumour cell-specific surface makers for positive selection or markers present in normal blood cells for negative selection. CellSearch, is the most widely used system based on the positive enrichment by immunoaffinity. It uses ferrofluid particles coupled to anti-EpCAM antibodies to enrich cells expressing the EpCAM epitope [15]. After enrichment, the system, stains enriched cells with 4′6-diamidino-2-phenylindole (DAPI) to allow detection of intact nucleated cells and with antibodies recognizing cytokeratin (CK) as positive CTC marker and CD45 as a negative (leucocyte) marker [16,17]. In 2004, the U.S. Food and Drug Administration cleared this system, for enumeration of CTCs in patients with prostate, breast and colorectal cancers. Other systems using similar approach are the IsoFlux, Adna Test, MagSweeper, EPISOT, CTC i-chip, MACS, CytoQuest CR system, etc. [18,19]. The other enrichment strategy is based on cell physical properties assumed to be different between the tumour and hematogenous cells, such as size, gravity, and polarity [20]. Some of the systems use filtration to enrich large tumour cells like ISET, Parsotrix, ScreenCELL, FAST disc. ClearCell also separates CTCs based on their size but for that it uses Dean and inertial forces created in a spiral microchannel to separate large cells in flow [21]. Another approach exploits dielectrophoresis (DEP) to separate neutral or polarizable particles such as CTCs in a non-uniform electric field [22].

Thus far, there is no platform for CTC enrichment able to deliver pure CTCs. Due to the fundamental distinct characteristics of the systems, each strategy has pros and cons [23]. Performance of CTC-enrichment systems is a compromise between the level or enrichment/depletion achieved and sensitivity to detect rare marker-positive cells. Selection of the best technology is dependent on the particular needs of the projects, namely: tumour entity, intended downstream use of the enriched CTCs, volume of sample, number/concentration of cells in the sample, flexibility towards use of different epitopes for enrichment, strategy for enumeration and level of throughput. Furthermore, the existing systems can differ greatly on their level of automation which ultimately influence the reproducibility of the assay. For example, in the CellSearch system, enrichment, immunostaining and analysis are performed on a semi-automated way while in systems as the Isoflux and Parsortix, and ClearCell, immunostaining needs to be performed manually.

In the particular case of pancreatic cancer, different studies have employed different systems for CTC detection with heterogenous results (Table 1).

Table 1. Clinical research on pancreatic cancers.

Reference	Year	Tumor Type	Number of patients	Platform	Principle of enrichment	CTC positivity
Okubo[13]	2017	PDAC	65	CellSearch	Immunomagnetic	33%
Michael G[12]	2021	PDAC	34	CellSearch	Immunomagnetic	71%
Bidard [24]	2013	PDAC	79	CellSearch	Immunomagnetic	11%
Dalvinder[25]	2020	NET	199	CellSearch	Immunomagnetic	44%
Hugenschmidt[11]	2020	PDAC	101	CellSearch	Immunomagnetic	6.8%
Kurihara[26]	2008	PDAC	26	CellSearch	Immunomagnetic	42%
Tao[27]	2019	PDAC	100	CR system (microfluidic chip)	Immunomagnetic	76%
Katharina[28]	2018	PDAC	69	MACS	Immunomagnetic	34%
Khoja [29]	2011	PDAC	54	CellSearch (#1) and ISET (#2)	Immunomagnetic and Size based	40% #1 90% #2
Earl[30]	2015	PDAC	35	CellSearch and MACS	Immunomagnetic	20%
Gementzis[31]	2018	PDAC	200	ISET	Size based	96%
Kulemann[2]	2017	PDAC	58	ScreenCell (filtration)	Size based	68%
Hyemin[32]	2021	PDAC	52	FAST disc (Flow filtration)	Size based	92%
Song[33]	2021	PDAC	31	Microfabricated porous filter	Size based	62.5%

PDAC- Pancreatic ductal adenocarcinoma
NET - Neuroendocrine tumour

Several CTC studies in pancreatic cancer described a relatively low recovery rate by the EpCAM-dependent enrichment methods (e.g. CellSearch) [24,26,29]. This seems consistent with the heterogeneous [29], and low EpCAM expression detected at the surface of tumour cells in pancreatic tumours [34,35]. Furthermore, the expression of this epitope can fluctuate as CTCs can be frequently found in different epithelial-to-mesenchymal transition states [36–38] and data from xenograft models suggest that EpCAM can become rapidly downregulated when cancer cells enter the bloodstream [39]. This dynamic diversity of EpCAM expression creates challenges for CTC enrichment by immunoaffinity, but systems as the CellSearch offer very limited possibilities to use alternative (or combination of) epitopes. As alternative to EpCAM, Mucin1 (MUC-1) epitope was already tested for immunoaffinity-based enrichment[35]. Overexpression of MUC-1 is observed in several types of tumour tissues, including in pancreatic tumours, and MUC-1 has been used as a biomarker for diagnosis and a target for therapy [40,41]. MUC-1 was already investigated in CTCs and the results suggest that in pancreatic [42], but also in ovarian [43,44] and metastatic breast cancer [45], MUC-1 distinguishes subtypes of CTCs different from those identified by using EpCAM. Furthermore, the presence of MUC-1pos/EpCAMpos CTCs in patients with pancreatic cancer has been shown to be associated with shorter OS [46]. Because of the diverse EpCAM expression in pancreatic cancer and the reduced validity of MUC-1-expressing CTCs, several CTC research groups have tested filters or other physical methods (that do not rely on epitope expression on the cell surface) for CTC enrichment in pancreatic cancer [29,30,47]. Collectively, the recovery rates of such methods seem superior. However, it is important to stress that the malignant origin of the detected cells remains largley unknown since filter-based platforms with strongly attached cells commonly do not permit downstream molecular analyses of individual cells. On one other hand, filter enrichment methods have limited application to enrich CTCs that are similar in size or even smaller to leukocytes.

The diversity of the existing systems suggest that optimized solutions for CTC detection could result from combining different methods that could compensate for each other's limitations [48]. Unfortunately, most of the devices for CTC enrichment are expensive, which hinder solutions combining two or more platforms. Although CTCs have a potentially large economic value, cost-effective methods are still needed to promote CTC research and to foster its implementation in the clinics.

1.2.2 – IsoFlux system

The IsoFlux^{TM} system (Fluxion Biosciences Inc., CA, USA), is a commercially available microfluidic platform for immunomagnetic-based enrichment of CTCs [49]. Before loading the sample in the system, cells are pre-incubated with magnetic beads coupled with antibodies and the sample is loaded in a reservoir that is connected to a microfluidic channel. The system applies pressure in the sample reservoir to push the sample through the channel at a controlled flow rate. A magnet placed on the top of the microchannel captures the magnetic beads and bound cells, while the rest of the sample (non-enriched cells) continues flowing in the microchannel and is collected in a separate reservoir. The enriched fraction, attached to the magnet, can ultimately be collected and subsequently analysed. For enumeration of CTCs among the co-enriched hematogenous cells, after enrichment, the resulting cell fraction still needs to be immune-stained and this process is done off-system, fully manually. As result, the protocol requires highly experienced operators doing the staining and identifying and counting cells after enrichment. Likewise, the fine microchannel in the system, and the flow conditions are specifically designed for standard blood samples (of 7.5 mL) and the system runs a fixed protocol which cannot be adapted.

Previous studies suggest that IsoFlux^{TM} can be particularly effective for enriching breast and prostate tumour cell line cells [49,50]. Several studies have reported that IsoFlux has higher efficiency compared to CellSearch for enriching CTCs from patients with prostate cancer, hepatocellular carcinoma [51], bladder cancer [52], and colorectal cancer [53,54]. Magnetic beads available from Fluxion can be self-conjugated with one's preferred antibody (the IsoFlux rare cell enrichment Kit (IsoRCEK) and that provides good opportunities to test different epitopes for enrichment, such as VAR2CSA for breast cancer [55].

1.2.3 – KingFisher system

The KingFisher^{TM} Sample Purification System (Thermo Fisher Scientific Inc., MA, USA), is a system initially conceived for magnetic-based nucleic acid purification that can also be used for immunoprecipitation and protein purification [56,57].

The KingFisher system operates with a row of 12 magnetic rods that can move up- and down immersing on a 96-well deep well-plate to mix samples, and to collect and transport beads from one well to the next. The magnetic beads capture targeted ligands and the transport through multiple wells can be used to perform ligand's enrichment, purification, concentration, and labeling/stainnig with a standardized set program. So far, application of the KingFisher instrument to enrich CTCs has not been reported and there are no protocol described for that. However, this system it is fully open and allow the design of new protocols, where various magnetic beads (and consequently various epitopes) can be used and where the enrichment can be even combined with the subsequent staining steps. Unlike CellSearch or IsoFlux, the programme can be fine-tuned to match the needs of different types of magnetic beads and samples. The volume capacity of the wells is 1mL and in this format, the system can process 12 samples in parallel (12 mL sample volume). However, the system accommodates two deep well-plates so it can be programmed to process automatically a total of 24 samples. Furthermore, the system can be adapted to operate with two 24-well deep-well plates (each well allowing a maximum of 5 ml) using instead a row of 6 giant concatenation magnetic rods which further increases the total volume of sample that can be processed (up to 60 mL). This suggested throughput of the KingFisher system is far greater than those of other platforms. Another important point is that the enrichment can be integrated with immunostaining in one single automated protocol reducing the human operator errors and improving reproducibility.

1.3 –DLA

The major obstacle in CTC isolation is their extreme rarity [16,58]. This raises questions if the low detection rates, particularly in localized stages of the disease, are due to the lack of cells migrating into the blood stream or because the relatively low sample volume (typically 7.5mL) compared to the whole circulating blood [58]. Fischer et al. proposed that the diagnostic leukaphaeresis (DLA) method can be used to increase dramatically the volume of blood that can be screened from the patients therefore increasing the number of CTCs detected in samples [59–62]. DLA is a shorter version of leukapheresis, a standard medical procedure long in use for several applications [63]. Its principle is to separate the different components in the blood by continuous centrifugation, collect the required components such as the white blood cells, and return the remaining blood components to the patient at the same time. Typically, the fraction targeted by DLA are the mononuclear cells (MNCs) and therefore as result of the procedure, it is obtained a product highly concentrated in MNCs from peripheral blood. MNC concentration in DLA products is typically 30 times more than in peripheral blood [58,60] and the total number of MNCs typically contained in one DLA product is equivalent to approximately 2.5L of blood, far above of the volume of blood normally screened for CTC examination (7,5 mL). The premise of using DLA to concentrate CTCs is that the density of CTCs is similar to that of MNCs, which seems to be the case [58]. Several studies have already reported CTC detection in DLA products. All of them report much higher detection rates and number of CTCs detected in DLA compared to normal peripheral blood samples [21,60,62,64,65]. With CellSearch system, CTC detection increased up to 32 times using DLA compared to 7.5 mL of blood despite only a small fraction of the DLA product (~5%) can be investigated with the actual existing protocols [65]. Estimations indicate that the whole DLA sample should have about 205 times more CTCs than the 7.5 ml peripheral blood sample [62], especially for metastasized patients. Interestingly, if DLA was filtered using a 5 μm pore microsieve, a large loss of CTCs was observed [60], demonstrating the challenge imposed by these highly concentrated products for filtration-based methods.

1.4 – Ethical clearance

All experiments were performed with the approval of the Local Ethics Committee of Medical Faculty of the Heinrich-Heine-University Düsseldorf, Germany (N. 4446). The experiments were performed in accordance with the relevant guidelines and regulations and ethical principles of the Declaration of Helsinki.

1.5 – Aims of the thesis

The capacity to detect CTCs is severely hampered by their rarity and low number in standard blood samples. Several devices and workflows have been reported for the enrichment and identification of CTCs, but they were designed to be used with standard blood samples (~7.5 mL), and their performance with highly concentrated DLA products is unclear. In the present work, we aimed to validate protocols using the IsoFlux and KingFisher platforms for magnetic-based enrichment of rare cells in DLA samples. More concretely, the main objectives for this work are as follows:

1- Explore different cell membrane epitopes for positive isolation of rare cells of pancreatic cancer origin. For this, we will compare the expression of different epitopes on the tumour cell surface and their performance for the specific purpose of magnetic-based tumour cell enrichment in DLA samples.

2- Adapt and design new protocols to analyse DLA samples with the IsoFlux and KingFisher systems.

3- Investigate the performance of different magnetic beads for enrichment of rare tumour cells from DLA samples with the KingFisher and IsoFlux systems. For that, we will compare magnetic beads differing in size and conjugation for the enrichment and detection of rare pancreatic tumour cells from DLA products.

2 –PUBLISHED ORIGINAL PAPER

cancers

MDPI

Article

Magnetic-Based Enrichment of Rare Cells from High Concentrated Blood Samples

Junhao Wu [1], Katharina Raba [2], Rosa Guglielmi [1], Bianca Behrens [1], Guus Van Dalum [1], Georg Flügen [1], Andreas Koch [3], Suraj Patel [4], Wolfram T. Knoefel [1], Nikolas H. Stoecklein [1,*] and Rui P. L. Neves [1,*]

1 Department of General, Visceral and Pediatric Surgery, University Hospital and Medical Faculty of the Heinrich-Heine University Düsseldorf, Moorenstr. 5, 40225 Düsseldorf, Germany; JunHao.Wu@med.uni-duesseldorf.de (J.W.); Rosa.Guglielmi@med.uni-duesseldorf.de (R.G.); Bianca.Behrens@med.uni-duesseldorf.de (B.B.); vandalum@gmail.com (G.V.D.); georg.fluegen@med.uni-duesseldorf.de (G.F.); WolframTrudo.Knoefel@med.uni-duesseldorf.de (W.T.K.)

2 Institute for Transplantation Diagnostics and Cell Therapeutics, University Hospital and Medical Faculty of the Heinrich-Heine University Düsseldorf, 40225 Düsseldorf, Germany; Katharina.Raba@med.uni-duesseldorf.de

3 Thermo Fisher Scientific, Postfach 200152, Frankfurter Str. 129B, 64293 Darmstadt, Germany; andreas.koch@thermofisher.com

4 Thermo Fisher Scientific, 3 Fountain Drive, Inchinnan, Renfrew PA4 9RF, UK; suraj.patel@thermofisher.com

5 * Correspondence: nikolas.stoecklein@med.uni-duesseldorf.de (N.H.S.); rui.neves@med.uni-duesseldorf.de (R.P.L.N.); Tel.: +49-211-81-04109 (N.H.S.); +49-211-81-04502 (R.P.L.N.)

Received: 2 March 2020; Accepted: 8 April 2020; Published: 10 April 2020

Abstract: Here, we tested two magnetic-bead based systems for the enrichment and detection of rare tumor cells in concentrated blood products. For that, the defined numbers of cells from three pancreatic cancer cell lines were spiked in 10^8 peripheral blood mononuclear cells (PBMNCs) concentrated in 1 mL, mimicking diagnostic leukapheresis (DLA) samples, and samples were processed for circulating tumor cells (CTC) enrichment with the IsoFlux or the KingFisher systems, using different types of magnetic beads from the respective technology providers. Beads were conjugated with different anti-EpCAM and MUC-1 antibodies. Recovered cells were enumerated and documented by fluorescent microscopy. For the IsoFlux system, best performance was

obtained with IsoFlux CTC enrichment kit, but these beads compromised the subsequent immunofluorescence staining. For the KingFisher system, best recoveries were obtained using Dynabeads Biotin Binder beads. These beads also allowed one to capture CTCs with different antibodies and the subsequent immunofluorescence staining. KingFisher instrument allowed a single and streamlined protocol for the enrichment and staining of CTCs that further prevented cell loss at the enrichment/staining interface. Both IsoFlux and KingFisher systems allowed the enrichment of cell line cells from the mimicked-DLA samples. However, in this particular experimental setting, the recovery rates obtained with the KingFisher system were globally higher, the system was more cost-effective, and it allowed higher throughput.

Keywords: circulating tumor cells; immunomagnetic enrichment; concentrated blood products; diagnostic leukapheresis; IsoFlux; KingFisher

1. Introduction

A growing body of evidence suggests that circulating tumor cells (CTCs), i.e., tumor cells shed into the circulation by solid tissues, have the potential to be used as biomarkers for clinical monitoring and as a source of information to better understand the complex metastatic cascade [1,2]. However, assessing the full clinical and biological informative value of CTCs has remained very challenging due to their rarity [3,4]. Considering that typically only 1–10 CTCs are present in 1 mL of blood [4], the low blood volume of standard blood samples (7.5–10 mL) strongly contributes to the low detection frequency [5]. Diagnostic leukapheresis (DLA) is a powerful approach to sample liters of blood [6] improving significantly the frequency and numbers of detected CTCs [6–9]. DLA is based on a continuous flow centrifugation of peripheral blood leading to a density-based separation of the cellular fractions which can be selectively harvested. The principle underlying application of DLA to enrich CTCs is that CTCs have a similar density and can be harvested together with the faction of peripheral blood mononuclear cells (PBMNCs) from patients [4]. As a result, DLA products typically contain a concentration of PBMNCs that is >25× higher than the one found in peripheral blood. This is currently the major challenge to effectively utilize the full power of DLA for CTC detection and isolation [4,7].

Most commonly, CTC-detection relies on the immunomagnetic enrichment of cells expressing epithelial cell adhesion molecule (EpCAM) [10], followed by the immunofluorescence detection of cytokeratin (CK) positive and CD45 negative nucleated ($CK^{pos}/CD45^{neg}/DAPI^{pos}$) cells [3,11]. This is the basis of the CellSearch system [12,13], the only FDA-cleared system for CTC enrichment and which we and others have previously demonstrated to be efficient to process DLA samples [6–9]. However, the throughput for DLA is limited [4] and the enrichment of CTCs from epithelial malignancies is restricted to EpCAM [14]. One alternative technology for positive CTC enrichment is the IsoFlux system (Fluxion Biosciences Inc., Alameda, CA, USA) [15], to our best knowledge the only semi-automated bead-based immunomagnetic system commercially available. IsoFlux was demonstrated to be effective for EpCAM-based enrichment of breast, prostate [15], and colorectal [16] cell line cells, and CTCs from patients with prostate [15,17], hepatocellular carcinoma [18], and bladder cancer [19]. This microfluidic platform offers some flexibility, since magnetic streptavidin-conjugated beads are available to broaden the spectrum of epitopes that can be used for enrichment. However, the staining of enriched cells for CTC-detection is performed manually, which can be disadvantageous for the reproducibility and throughput of the system. In the present work, we compared the performance of this system to enrich tumor cells from samples mimicking DLA products with the one from the KingFisher Duo Prime Purification System (Thermo Fisher Scientific Inc., Waltham, MA, USA), an instrument present in the market for magnetic-based nucleic acid purification [20] immunoprecipitation and protein purification [21], but which was never reported for isolation of rare cells. The instrument uses permanent earth magnetic rods to transfer magnetic bead-bound samples through successive solutions according to user-defined programs, and its specifications suggested to us that the system could also be used for enrichment of CTCs. Moreover, the specifications also suggested that different epitopes and magnetic beads could be used, and that enrichment and staining steps could be combined in one single automatic protocol, possibilities that, combined, are not available in any commercial system for CTC enumeration.

The use of different epitopes for CTC enrichment is of particular interest in the case of tumors as pancreatic ductal adenocarcinomas (PDAC), in which the level of EpCAM expression is particularly heterogeneous [22] and low in approximately 50% of the cases [23,24]. This may explain the relative low number [22,25,26] and frequency [25] of CTCs

detected with EpCAM-based assays, particularly when compared to other metastatic diseases [13] and to EpCAM-independent assays [22,27,28]. Aiming at strategies to overcome the limitation of using EpCAM as single epitope for enrichment of CTCs, we tested both IsoFlux and KingFisher systems using different EpCAM- and Mucin1 (MUC-1)-coupled magnetic beads to enrich pancreatic tumor cells. MUC-1 is a transmembrane glycoprotein, which is highly expressed in the majority of pancreatic tumors [29], and that was already proposed as a therapeutic target [30,31]. A previous work has shown that high numbers of MUC-1^{pos}/EpCAM^{pos} CTCs correlate with shorter overall survival in patients with pancreatic cancer [32], and data suggest that MUC-1 and EpCAM might identify different subtypes of CTCs in pancreatic [33], but also in ovarian [34,35] and metastatic breast cancer [36].

2. Results

2.1. Epitope Expression in Model Cells Lines

To analyze the suitability of model cells for enrichment experiments, we investigated three different human pancreatic cancer cell lines for their EpCAM and MUC-1 surface expression (Figure 1). Based on the levels of the epitopes detected, we have classified the pancreatic line HuP-T4 line as EpCAM^{High}/MUC-1^{Low}, the CAPAN-1 line as EpCAM^{Mid}/MUC-1^{High}, and the MIAPACA-2 line as EpCAM^{Low}/MUC-1^{Neg}. Strikingly, the number of epitopes that we could detect with the Anti-EpCAM VU1D9 clone was higher than with the clone BerEP4. Clear MUC-1 expression could only be detected on CAPAN-1 cells and the number of epitopes detected by the two clones tested did not differ considerably (Figure 1).

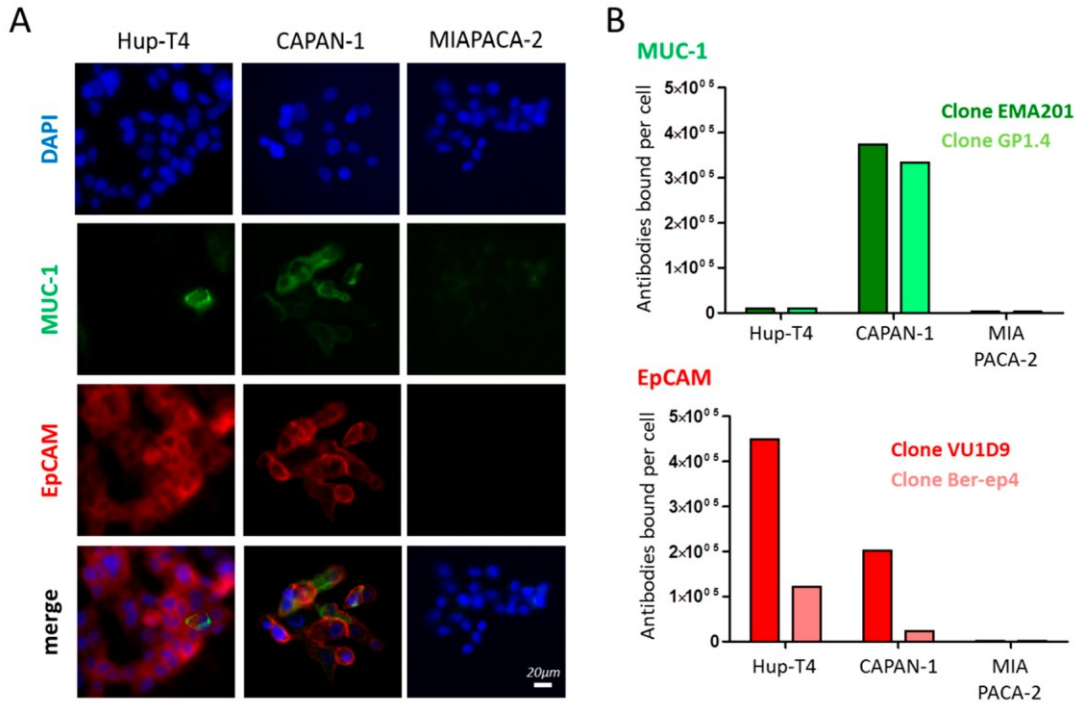

Figure 1. MUC-1 and EpCAM expression in HuP-T4, CAPAN-1 and MIAPACA-2 pancreatic cells lines. (**A**) Immune-fluorescence microscopy analysis of EpCAM and MUC-1 expression. (**B**) Number of epitopes detected by two anti-MUC-1 clones (EMA201 and GP1.4), and two anti-EpCAM clones (VU1D9 and Ber-EP4) by flow cytometry.

2.2. Beads Used for Enrichment and Read-Out for Cell Enumeration

For enrichment in the Isoflux system, we used three different types of beads available from Fluxion (Iso-CEK, IsoRCEK, and Iso-RCEK-SA) and according to the instructions provided by the manufacturer (Table 1). As no protocols or standards were available for enrichment in the KingFisher system, we tested four different types of beads available from Thermo Fisher Scientific (Dy-EpE, Dy-ACK, Dy-BioB, and Pi-Strep) and tested three different amounts of those beads (minimal (MIN), middle (MID) and maximal (MAX)) (Table 1).

We defined the MIN amount as the number of Thermo Fisher beads, providing the same surface area as the Iso-CEK beads in the standard IsoFlux CTC Enrichment Kit assay. Using flow cytometry, we determined the size of the Iso-CEK beads as 4.2 µm (See Figure S1) and analyzing their spectrophotometric characteristics, we estimated that 10.98×10^5 beads are present in the 40 µL of bead suspension used per sample in the IsoFlux CTC Enrichment Kit assay (See Figure S2). Based on these values, we calculated that the surface provided by these beads in the respective assay is 6.11×10^7 µm^2 (see Figure S2D) and determined the volume of Thermo Fisher beads necessary to achieve

that surface based on their sizes and concentrations given by the manufacturer. For each type of Thermo Fisher beads, we subsequently defined the middle (MID) amount of beads as 5× MIN, and the maximal (MAX) amount of beads as 10× MIN (see Table S1). These different amounts of beads were clearly distinct under the bright-field microscope light (Figure 2A), however they did not compromise the identification of fluorescent-labeled cells, even in areas of the slide-field where the concentration of beads was highest (typically the center of the sample field) (Figure 2B).

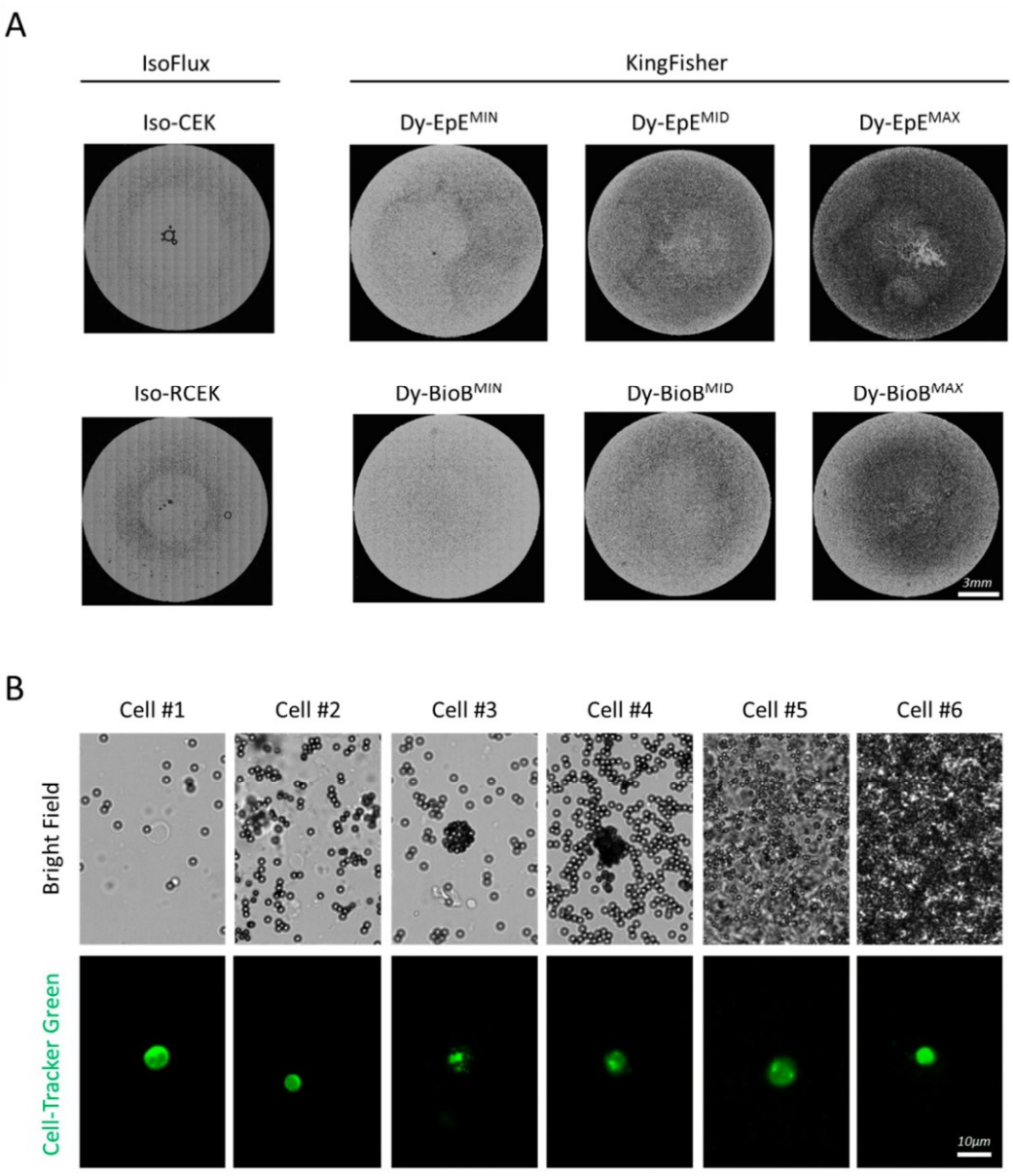

Figure 2. Identification of enriched pre-labelled cells among the beads. (**A**) Distribution of Iso-CEK, Iso-RCEK, Dy-EpE^{MIN,MID,MAX} and Dy-BioB^{MIN,MID,MAX} beads in field of a three-field microscope slide used for enumeration of enriched cells. Each image is a montage of all 357 tiled bright field images covering the complete field. (**B**) Six individual cells identified in one same sample enriched with Dy-EpE beads.

Table 1. Beads used for enrichment on the IsoFlux and KingFisher systems.

Type of Beads		IsoFlux			Thermo Fisher			
		Iso-CEK	**Iso-RCEK**	**Iso-RCIK-SA**	**Dy-EpE**	**Dy-ACK**	**Dy-BioB**	**Pi-Strep**
Commercial name		CTC Enrichment Kit	Rare Cell Enrichment Kit	Rare Cell Isolation Kit SA	Dynabeads Epthelial Enrich	Dynabeads Antibody Coupling Kit	Dynabeads BiotinBinder	Pierce Streptavidin Beads
Diameter (µm)		4.2 *	4.2 *	3.0 *	4.5	2.8	2.8	1
Concentration (beads/mL)		0.27 **	n.a.	n.a.	4×10^8	6.7×10^8	4×10^8	96×10^8
Coupling		Pre-coupled with anti-EpCAM Ab	For coupling with mouse IgG antibodies	For coupling with Biotin-conjugated Abs	Pre-coupled with anti-EpCAM Abs	For coupling via covalent binding	For coupling with Biotin-conjugated Abs	For coupling with Biotin-conjugated Abs
Coupled clone	EpCAM	n.a.	BerEP4 VU1D9	VU1D9	BerEP4	VU1D9	VU1D9	VU1D9
	MUC-1	-	EMA201 GP1.4	Not tested	-	Not tested	GP1.4	Not tested
Amount of beads	According to protocol	40µL	50µL	62.5µL	-	-	-	-
	MIN	-	-	-	2.4 µL	3.7 µL	6.2 µL	2 µL
	MID	-	-	-	12 µL	18.5 µL	31 µL	10 µL
	MAX	-	-	-	24 µL	37 µL	62 µL	19.9 µL

n.a.—Information not available. *— Information determined experimentally (Please see Figure S1). **- Information determined experimentally (Please see Figure S2). Amount of beads refers to the volume of the commercially available bead suspensions as provided by the manufacturer which was used per sample.

2.3. EpCAM-Based Enrichment of Spiked Cells

After proving the suitability of the mimicked-DLA products to model patient-derived DLAs [37] and defining different amounts of beads for enrichment, we challenged the IsoFlux and KingFisher systems for EpCAM-based enrichment of pancreatic cells pre-labeled with CellTracker Green spiked in mimicked-DLA products (Figure 3). The IsoFlux system was used with its standard enrichment program, while for the KingFisher system we designed a first protocol with one enrichment and one washing step, the WuDuo1 program (See Figure S3).

Using both systems, we could recover cells from the three pancreatic lines, and for each bead type used the recoveries were globally concordant with the level of EpCAM expression in the cells: HuP-T4 cells were most efficiently recovered, followed by CAPAN-1 and lastly by MIAPACA-2 (Figure 3A). The highest mean recoveries of HuP-T4 and CAPAN-1 cells were obtained in the KingFisher system with Dy-EpE beads and Dy-BioB beads, respectively (Figure 3A, B). In both cases, these mean recoveries were in line or even higher than the ones that we obtained with the CellSearch system (See Figure S4). No statistically significant differences could be detected between recovery rates obtained using the MID and MAX amounts of beads (Figure 3). In the IsoFlux system, Iso-CEK and Iso-RCEK-BerEP4 beads were the ones with more consistent results. Interestingly, the recoveries with Iso-RCEK-BerEP4 beads were consistently

higher than recoveries with the Iso-RCEK-VU1D9, despite the higher abundance of the VU1D9 epitope on the cells (Figure 1).

Based on these results, we further tested the Iso-CEK, Iso-RCEK-BerEP4, Dy-EpEMID, and Dy-BioBMAX-VU1D9 beads, to recover different amounts of HuP-T4 and CAPAN-1 cells spiked in mimicked-DLA samples (1–100 cells) (Figure 3B). Additionally, in this set of experiments, the recovery of HuP-T4 cells (43%–78%) was globally more efficient than CAPAN-1 cells (34%–52%) (see Figure S5), and with the exception of one measurement with Dy-BioBMAX-VU1D9 (100 cells), higher recoveries were obtained using the Dynabeads in the KingFisher system. Importantly, in the range tested, the recoveries for both CAPAN-1 and HuP-T4 lines in both systems were close to linearity (R2 of linear regression were between 0.8411 and 0.9913) (see Figure S5).

Notably, the EpCAM-based enrichment of CAPAN-1 cells was differentially influenced by cell preservatives. CellSave and TransFix fixatives positively influence the recovery in both systems, PFA 0.1% significantly decreased the recovery in both systems, and Streck tubes caused a striking reduction in recovery with Iso-CEK beads, but not with the Dy-BioB^{MAX}-*VU1D9* beads (see Figure S6). The positive effect of TransFix preservative could also be recapitulated in experiments using CAPAN-1 cells spiked in normal whole blood samples (see Figure S7A).

Using the Dy-BioB^{MAX}-*VU1D9* beads in the KingFisher system, we could also recover HCT-116, SW620 (both colorectal cancer) and SKBR-3 (breast cancer) cells, showing that the system can also be applied for other tumor entities (See Figure S7B). In additional experiments, in which we used Hoechst nuclear dye to also detect the WBCs co-enriched using the Dy-BioB^{MAX}-*VU1D9* beads and the WuDuo1 program in the KingFisher system, we detected, on average, 18061 WBCs. This indicates a depletion efficiency of 3.7 Logs, corresponding to a depletion of >99.98% of WBCs and it results in an estimated CTC purity of 0.188% (See Figure S8).

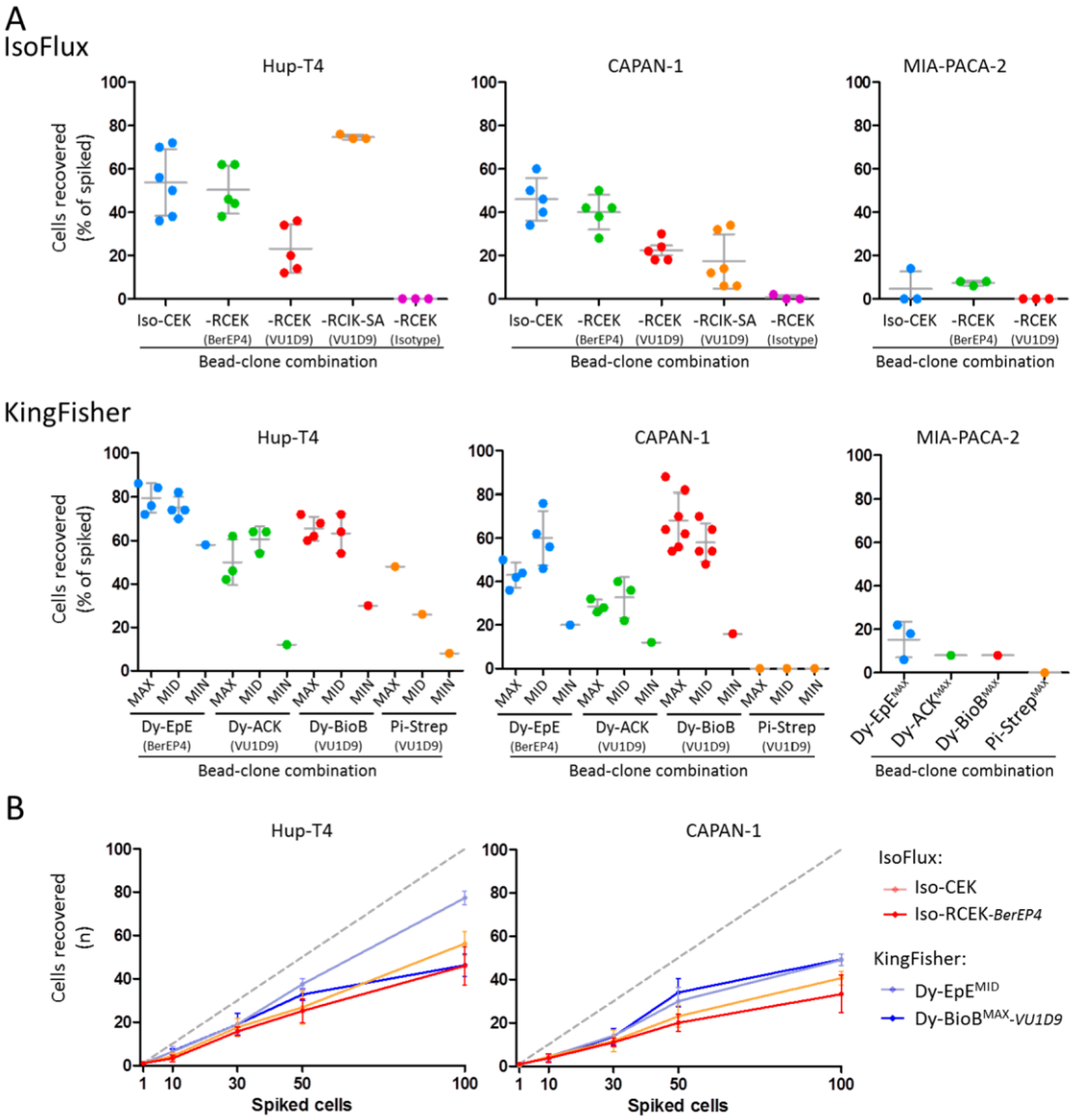

Figure 3. EpCAM-based recovery of HuP-T4, CAPAN-1 and MIA-PACA-2 cells spiked in mimicked-DLA products. (**A**) Recovery of 50 pre-labeled cells from the three lines using the IsoFlux system and three types of beads available from Fluxion (Iso-CEK, Iso-RCEK, and Iso-RCIK-SA) (upper panels) and using the KingFisher Duo system running the WuDuo1 program three different amounts ("MAX", "MID" and "MIN") of four types of beads available from Thermo Scientific (Dy-EpE, Dy-ACK, Dy-BioB, and Pi-Strep) (lower panels). (**B**) Recovery of different numbers of spiked pre-labeled HuP-T4 and CAPAN-1 cells using Iso-CEK and Iso-RECK-*BerEP4* beads in the IsoFlux system, and Dy-EpE^{MID} and Dy-BioB^{MAX}-*VU1D9* beads in the KingFisher Duo system.

2.4. Alternative Strategies for Enrichment of CTCs with the KingFisher System

We tested MUC-1 as an alternative or additional marker for the enrichment of pancreatic cells using Dy-BioB^{MAX} and Iso-RCEK beads in their respective systems (Figure 4).

Interestingly, exclusively MUC-1-based recovery rates were consistently and significantly lower compared to those previously obtained with the same beads coupled with the VU1D9 or BerEP4 anti-EpCAM clones (Figure 4A). This is more surprising given the higher number of MUC-1 epitopes compared to EpCAM in CAPAN-1 cells (Figure 1). Combining MUC-1- and EpCAM-coupled beads in the same enrichment step (simultaneous enrichment), we could only partially increase the recovery rate. Yet, more interestingly, using the WuDuo2 protocol, it was possible to perform sequential MUC-1and EpCAM-based enrichments in the KingFisher, and thus achieve global recovery rates similar to the ones obtained with EpCAM alone, while capturing two separate populations of cells (Figure 4B). Taking advantage of the flexibility of the KingFisher system, we have also tested the recovery rate of CAPAN-1 cells performing CD45 depletion, followed by EpCAM-based enrichment in a single automated protocol (See Figure S9). Despite achieving a reduction of the number of background mono nuclear cells of almost 80% with the initial CD45-based depletion, we could not improve the subsequent recovery rate of CAPAN-1 cells.

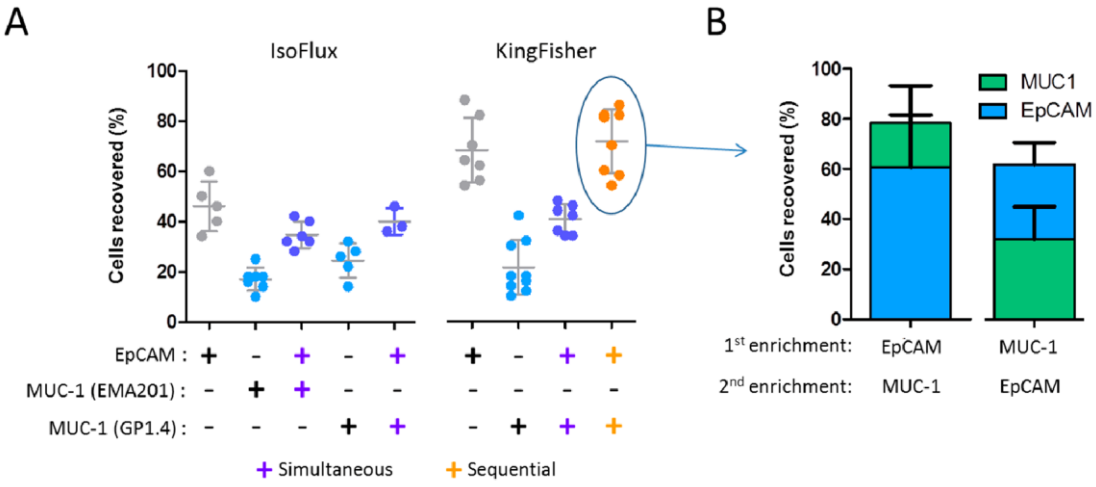

Figure 4. MUC-1 alone and MUC-1/EpCAM combined recovery of CAPAN-1 cells spiked in mimicked-DLA products. (**A**) (Left panel) Recovery of 50 pre-labeled CAPAN-1 cells with Iso-RCEK beads coupled with anti-MUC-1 clones EMA201 and GP1.4 alone or in combination (simultaneous) with anti-EpCAM coupled beads using the IsoFlux system. For the simultaneous MUC-1 and EpCAM recovery, half of the amount of each bead type was used, so that the total amount of beads in the experiment was according to the original protocol. Data in grey are the same as in Figure 2. (Right panel) Recovery of 50 pre-labeled CAPAN-1 cells with Dy-BioB beads coupled with the GP1.4 clone alone or in combination (simultaneously and sequentially) with Dy-BioB anti-EpCAM coupled beads using the KingFisher Duo system. For the simultaneous MUC-1 and EpCAM recovery, half of the amount of each bead type was used, so that the total amount of beads in the experiment was the same as described in the material and methods (Dy-BioB^{MAX}). Data in grey are the same as in Figure 2. (**B**) Recovery of 50 pre-labeled CAPAN-1 cells after sequential EpCAM- and MUC-1-based enrichment in the KingFisher system.

2.5. Staining of Enriched Cells

Next, we tested the impact of the staining procedure necessary for CTC enumeration in clinical samples after enrichment (Figure 5).

Simulating the staining according to the IsoFlux Circulating Tumor Cell Enumeration Kit protocol, but using cells pre-labeled with CellTracker Green, we observed an additional reduction of 52% in the mean recovery of CAPAN-1 cells (from 46% to 22%, $p = 0.0078$ Mann–Whitney test), while a staining step introduced in the KingFisher WuDuo1 protocol (WuDuo1S protocol) led to a much milder reduction of 24% (from 68% to 52%, $p = 0.0864$ Mann–Whitney test) (Figure 5A). Interestingly, the introduction of this staining step, in which the cells are passed by one more solution than in the previous WuDou1 protocol, substantially reduced the number of WBCs co-enriched to a mean of 7588. This increased the depletion efficiency to 4.1 Logs, corresponding to a depletion of >99.99% of WBCs and consequently had a positive impact in the estimated purity (0.346%) (see Figure S8).

Notably, when antibody-based staining was effectively performed, we observed an increase in the fluorescence intensity of the Iso-CEK, Iso-RCEK-*VU1D9*, and Dy-EpE beads itself, particularly in the AF647-CD45 channel, suggesting that these beads retain capacity to unspecifically capture the staining antibodies (Figure 5B). Although the identification of CK^{pos} events was still possible, capturing of the staining antibodies by the beads created major difficulties to reliably exclude the presence of CD45 staining from those events and even to identify hematogenous cells expected to be $CD45^{pos}$. Capturing of the antibodies by these beads could be further validated by flow cytometry (see Figure S10). The exception was Dy-BioB beads, for which no binding of staining antibodies was observed by microscopy and flow cytometry, as expected, due to the fact that coupling to the Dy-BioB beads is dependent on biotin and this is not present in any of the staining antibodies.

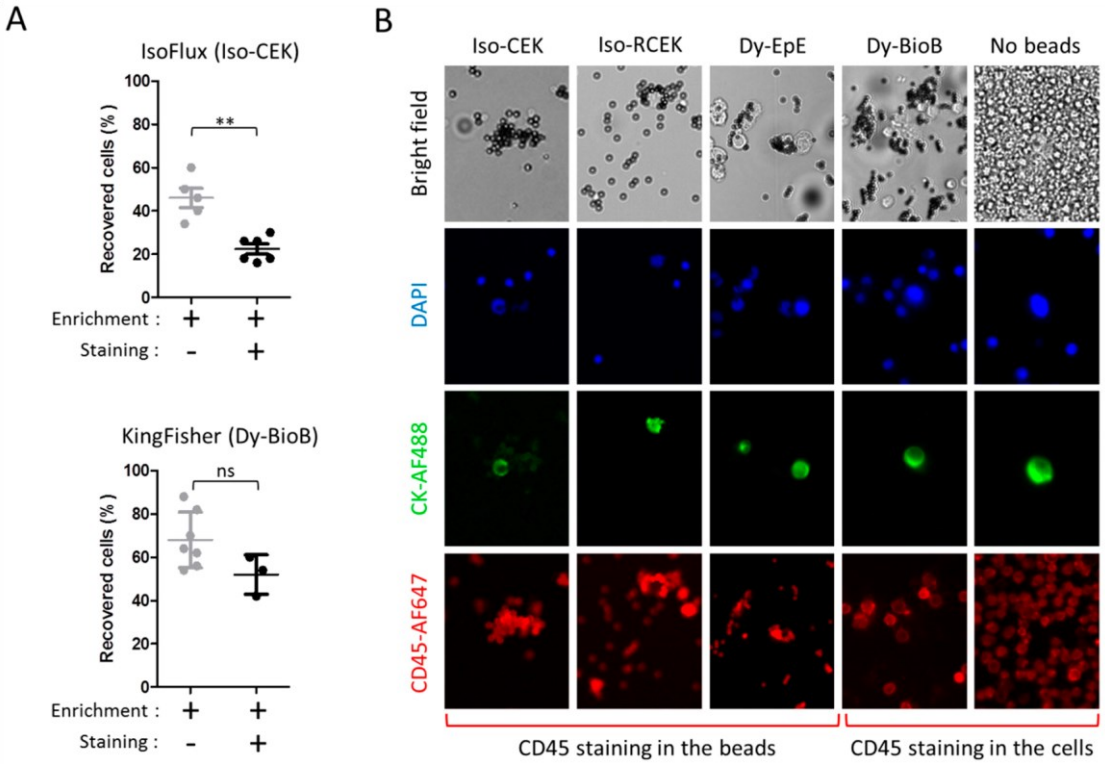

Figure 5. Impact of staining in the recovery and identification of cells spiked in mimicked-DLA products. (**A**) Impact of the staining procedure. *(Upper panel)* Recovery of 50 pre-labeled CAPAN-1 cells with Iso-CEK beads, with and without the subsequent staining procedure performed according to the IsoFlux protocol. For this experiment, the fluorescent-conjugated antibodies in the respective protocols were replaced by non-conjugated mouse IgG isotype control. *(Lower panel)* Recovery of 50 pre-labeled CAPAN-1 cells with Dy-BioB^{MAX} beads, with and without a subsequent staining procedure performed automatically in the KingFisher (protocol *WuDuo Staining*). (**B**) Impact of beads in the immunofluorescence identification of spiked and hematogenous cells. Cells enriched with the Iso-CEK, Iso-RCEK, Dy-EpE, and Dy-BioB beads were stained with DAPI, and AF488-conjugated CKs, and AF647-conjugated CD45 mouse monoclonal antibodies.

3. Discussion

Although DLA allows sampling liters of blood from tumor patients significantly augmenting CTC yield [6–8], the excess of WBCs in DLA products is challenging for effective CTC detection and currently limits the volume of DLA product that can be used. Previously, we have demonstrated upon analysis of only 2 mL with the CellSearch system, that DLA products contain higher concentrations and numbers of CTCs than those found in standard blood samples [6,8], and in a multicenter European study, we have started to uncover the potential of analyzing larger volumes of product [7]. An analysis of the complete DLA product (typically >40 mL) could provide an unprecedented opportunity to obtain enough CTCs for a more systematic molecular and functional characterization of the systemic disease towards a real liquid biopsy [7]. The fractioning of DLA products

for the parallel processing of multiple aliquots is not practically or economically viable, considering the actual costs per assay of the so far described technologies. Therefore, workflows allowing the cost effective and higher throughput processing of highly concentrated DLA products are of great need. In this context, we have evaluated the technical performance of IsoFlux and KingFisher systems to process samples mimicking DLA products containing spiked pancreatic cell line cells. These two systems are, to our best knowledge, the only systems available to perform the semi-automated magnetic-based positive enrichment of CTCs.

Globally, our work indicates that, although the enrichment of rare cells was possible with both systems, the efficiency of the KingFisher system is superior. This is notable, considering the fact that the KingFisher system was originally not designed for this purpose. The two systems differ considerably in their concept, which might explain the differences in performance. In the IsoFlux system, the sample experiences the magnetic field when flowing in a microfluidic channel. As the sample passes only once by the magnet, cells only have one (very short) opportunity to be collected. Differently, in the KingFisher, the sample is kept in a reservoir and the magnetic field is applied by a permanent earth magnetic rod that moves vertically through the sample in a defined number of times. In the basis of all protocols that we designed for the KingFisher, collection was done in three steps of 2'30' each (i.e., totally the sample is exposed to the magnet for 7.5 min in each collection step). This longer time will favor the capturing procedure. Although in the present work, we demonstrate the feasibility in 1mL samples, the low costs per sample of the KingFisher System (<20 EUR for one-bead type-based enrichment and <8 EUR for staining, according to current list prices), the possibility to run up to 12 aliquots in parallel under the same experimental conditions (scalable to 96 with the KingFisher Flex system), and the inclusion of automatic staining might open new perspectives for processing larger volumes of clinical DLA products.

One other unique feature of both IsoFlux and KingFisher systems is that they are flexible concerning the type of beads and the enrichment epitope. In a first step, we used EpCAM-based enrichment to compare the standard anti-EpCAM pre-coupled beads with self-coupled beads. Our results indicate that the recovery rates obtained with self-coupled beads can be similar to those of the pre-coupled counterparts, despite striking differences in the performance of the different self-coupled beads tested. In both systems, smaller beads (i.e., 3 μm Iso-RCIK-SA and 1 μm Pi-Strep beads) were generally less efficient at

capturing spiked cells, indicating the limitations of smaller magnetic particles for cell enrichment under the magnetic momentums of their respective magnets. Although the number of beads that can bind to one same cell is higher if the beads are smaller, the magnetic force exerted in each cell/beads complex is more strongly influenced by the diameter of the beads bound, which explains why larger beads, to a certain extent, allow higher recoveries of cells [38].

Using the KingFisher system, we could titrate the amount of beads per assay. The best results were obtained using 248×10^5 Dy-BioB beads (Dy-BioB^{MAX}), a number that is ~23 times higher that the number of beads used in the Isofux (See Table S1, Figure S3), and that provide a surface for contact that is 10× larger than that of the Isofux standard assay. This larger surface will favor the binding of beads to the cells. Typically, the conjugation of biotin groups to antibodies is done randomly, resulting in an unequal number and distribution of biotin groups over the antibody molecules. As coupling of the antibodies to beads happens via the biotin groups, the antibodies can be coupled to the DyBioB beads in orientations that hinder ligand binding. Moreover, biotinylation can even diminish the binding capacity of the antibodies, if its Fab regions become indeed biotinylated during this random process [39,40]. As an alternative to this random process, the use of site-specific antibody biotinylation of the Fc domain can maximize the accessibility of the Fab regions of antibodies coupled to surfaces [40]. This was previously demonstrated to increase the capturing of CTCs to a microfluidic chip [39], and to magnetic nanoparticles coated on a micro-sized immune-graphene oxide sheet [38], and we anticipate that the same could further improve CTC capturing capacities of DyBioB beads in the KingFisher system.

In general, recovery was in line with the level of EpCAM-epitope expression in the cells. Interestingly, using Iso-RCEK beads, we could obtain higher recoveries with the Ber-EP4 EpCAM antibody clone than with the VU1D9, despite the higher abundance of VU1D9 epitopes detected in the cell lines, which might indicate significant differences in the affinity of these two antibody clones [41]. Such differences in affinity have an impact on the strength of the bond between cells and beads [42], critical for pulling the cells towards the magnet. Our subsequent MUC-1-based enrichments further reinforce that idea. In PDAC, MUC-1 is an important cellular epitope, and in CAPAN-1 cells, it is much more abundant than EpCAM. Despite that, in both systems, recovery with MUC-1 was dramatically lower compared to that of beads coupled with EpCAM. However,

despite the low recovery, the possibility of capturing MUC-1 expressing CTCs seems of particular interest in samples of patients with tumors, as PDAC as assays based in EpCAM alone have resulted in the low number and frequency of CTCs [22,25,26]. Our results indicate that the sequential use of EpCAM and MUC-1 in the KingFisher might increase CTC yield and allow capturing different subpopulations of CTCs, which will deserve further investigation.

Interestingly, fixatives had an impact on the recovery of the spiked tumor cells. The challenge in fixation of samples resides in finding the right compromise between preserving the antigens
while maintaining their ability to be reached by antibodies [43]. Paraformaldehyde (PFA) is widely used for immunostaining (IS) (e.g., for fluorescence microscopy) (typically at 4%), but it has been demonstrated to cause loss of epitopes, to sterically hinder the access of the antibodies to their antigens, and the mislocalization of target proteins [44]. In addition, the more distal part of EpCAM molecule, recognized by VU1D9 and BerEP4 antibodies, has been shown to be degraded by protocols for immune histochemistry (IHC) of tissue sections involving formaldehyde fixation (typically at 4%, i.e., 10% Formalin solution) [45]. Although the concentration of PFA used in the present work (0.1%) is far below of that used for IS and IHC, partial degradation and masking of the EpCAM epitope by PFA can explain the drastic negative effect of this fixative on recovery of rare cells. The fixative contained on CellSave, TransFix and Streck tubes are proprietary and therefore their impact on cell recovery is difficult to interpret. However, the information available (e.g., from patent applications) suggests the use of formaldehyde releasers, which keep a concentration of formaldehyde high enough to stabilize cell morphology, but also low enough to mitigate the negative effect on the EpCAM epitope. The distinct effect of Streck fixative on the recovery with Iso-CEK and Dy-BioB-VU1D9 beads might result from the different impact of this fixative on the epitopes recognized by the antibodies coupled to these beads (information not available for the case of Iso-CEK beads). Collectively, our results indicate that the immunomagnetic recovery of rare cells in highly concentrated blood samples is determined by an assay specific combination of multiple factors, such as cell size, bead size, epitope expression, sample fixation, antibody affinity and magnetic field, which was more favorable in the case of the KingFisher system.

Similarly, to any other CTC enrichment technology, IsoFlux and KingFisher systems were not able to provide pure CTCs and many hematogenous cells were co-enriched. We have tested immunofluorescence staining to discriminate spiked tumor cells from the background cells, an essential step for CTC enumeration in clinical samples. In the IsoFlux system, this step is performed manually outside the platform. This extended the hands-on time and led to an additional 50% cell loss, which may limit the reproducibility of the technique and its applicability to larger studies. In the KingFisher system, the staining can be automated and integrated with enrichment in one workflow. This resulted in a more effective cell recovery and faster sample processing. Importantly, we have noticed that self-coupled Iso-RCEK beads, pre-coupled Iso-CEK and Dy-EpE beads extensively captured the antibodies used for staining, sequestering them from binding to the cells. The antibodies used here for immunofluorescence staining are mouse monoclonal antibodies (anti-panCK C11, anti-CK19 A53-B/A2, and anti-CD45 HI30) and were chosen due to their extensive clinical validation. These clones are the ones used in the CellSearch system [14], considered the gold standard and still the only system cleared by the Food and Drug Administration (FDA) for the in vitro diagnostic (IVD) enumeration of CTCs in patients. Further tests indicated that the binding of antibodies to Iso-CEK beads was dependent on the *Fc* fraction of mouse immunoglobulin G (IgG) (data not shown). Strategies to block antibody capturing by beads using different protein solutions could reduce, but not completely eliminate, the problem (data not shown), a fact that, from our perspective, limits the use of these beads and particularly the IsoFlux system for CTC enumeration purposes. Interestingly, as alternative to enumeration, immune-magnetically enriched CTCs can be detected with sensitive DNA- or RNA-based assays [46–48]. Similar assays were already successfully applied in cellular fractions enriched with IsoFlux [15,19,49] and with Dynabeads processed manually [50]. Such strategies overcome the difficulties faced for microscopic enumeration, although they do not allow the generating of individualized molecular profiles of the different CTCs.

4. Materials and Methods

4.1. Cell Lines, Cell Culture, and Preparation of Spiked Samples

Three pancreatic cancer cells, CAPAN-1, MIAPACA-2 and HuP-T4 were obtained from the Leibniz Institute DSMZ—German Collection of Microorganisms and Cell

Cultures (Germany). All cell lines were maintained in culture under standard conditions: CAPAN-1 were cultured in RPMI1640 (PAN-biotech, Aidenbach, Germany) supplemented with 20% fetal bovine serum (FBS) (Sigma, Steinheim, Germany); MIAPACA-2 in Dulbecco's MEM (PAN-biotech, Germany) supplemented with 20% FBS and 2.5% horse serum (PAN-biotech, Germany); and HuP-T4 in MEM Eagle (with EBSS, 2 mM L-Glutamine, 1 mM Sodium pyruvate, NEAA, and 1.5 g/L NaHCO3) (PAN-biotech, Germany), supplemented with 20% FBS. To prepare single-cell suspensions for experiments, cells were harvested from culture flasks using standard treatment with 0.05% Trypsin (PAN-biotech, Germany). For optimization of the CTC enrichment procedure, we used cells pre-labeled with CellTracker Green CMFDA Dye (Life Technologies, Carlsbad, CA, USA), according to the manufacturer's protocol. Subsequently, one, ten, or 30 dye positive cells were spiked manually, while 50 or 100 dye positive cells were spiked by flow cytometry using the MoFlo XDP flow cytometer (Beckman Coulter, Germany) into samples mimicking patient DLA products (mimicked-DLA products) (1 mL each sample). These mimicked-DLA products were prepared by isolating PBMNCs from the Buffy coats of healthy donors using Ficoll-Paque PLUS (d = 1.077 ± 0.001 g/mL; GE Healthcare, Sweden) density gradient centrifugation at 800× *g* for 20 min, subsequently washing the cells twice with PBS, and resuspending the cells to a concentration of 10^8 PBMNCs/mL, with PBS containing 0.5% BSA and 2 mM EDTA. Importantly, the cellular composition of these products was comparable with that of the patient-derived DLA products (see non-published material). All experiments were performed with the approval of the Local Ethics Committee of Medical Faculty of the Heinrich-Heine-University Düsseldorf, Germany (N. 4446). The experiments were performed in accordance with the relevant guidelines and regulations and ethical principles of the Declaration of Helsinki. Buffy coats were obtained from healthy blood donors, as anonymously provided by the blood donation center of the Institute for Transplantation Diagnostics and Cell Therapeutics, University Hospital Düsseldorf, Düsseldorf, Germany, with written informed consent for the use of surplus blood products for research purposes obtained from each blood donor. Date related to human samples were all analyzed anonymously.

4.2. Evaluation of MUC-1 and EpCAM Expression on Cell Lines

For the immune-fluorescence microscopy analysis of EpCAM and MUC-1 expression, cells were grown in an 8 well glass Lab-Tek Chamber Slide (Nunc, Rochester, NY, USA). For immune-staining, cells were washed once with PBS, incubated for 45 min with 200 µL of staining mix (AF488-conjugated anti-MUC-1 clone GP1.4 at 3.5 µg/mL (Novus, CO, USA), AF647-conjugated anti-EpCAM clone VU1D9 at 3.5 µg/mL (Cell Signaling Technology, Danvers, MA, USA), in PBS with 10% of AB-Serum (Bio-Rad Medical Diagnostics, Dreieich, Germany), and washed once with PBS. Following this, nuclear staining was performed with 200 µL of Hoechst 33342 reagent (Invitrogen, Eugene, OR, USA) at 2 µg/mL diluted in PBS and for 10 min at room temperature. Subsequently, the plastic media chamber was detached from the slide, the gasket was removed, 10 µL of Vectashield mounting medium (Vector Laboratories, Burlingame, CA, USA) was added to each field, and a coverslip was applied. Samples were scanned manually in an Eclipse E400 fluorescence microscope (Nikon, Tokyo, Japan), equipped with an automated XY stage controlled with home-built software, a 10x objective, a DAPI filter (Ex 377/50; Em 409/LP), a FITC filter (Ex 482/18; Em 520/28), an APC filter (Ex 640/30; Em 520/28), and a monochromatic camera. The exposure times were 10 ms for the detection of Hoechst, 200 ms for MUC-1-AF488, and 2000 ms for EpCAM-AF647. The images were analyzed using ICY software (http://icy.bioimageanalysis.org/) and the enumeration was done manually.

To determine the number of epitopes detected by two anti-MUC-1 clones (EMA201 and GP1.4), and two anti-EpCAM clones (VU1D9 and Ber-EP4) by flow cytometry, were used the BD Quantibrite Beads (BD Biosciences, San José, CA, USA). Measurements were taken according to the manufacturer's protocol. Briefly, 106 cells were resuspended in 750 µL of PBS containing 20% AB-Serum (Bio-Rad, Germany) and incubated for 20 min at 37 ˚C (to block unspecific Ab binding), centrifuged, and resuspended in 100 µL of PBS, containing 10% AB-serum and one of the following unconjugated primary mouse anti-human antibodies: Anti-MUC-1 clone EMA 201 at 2 µg/mL (Abnova, Taipei, Taiwan, China); Anti-MUC-1 clone GP 1.4 at 2 µg/mL (Invitrogen, Carlsbad, CA, USA); Anti-EpCAM clone VU1D9 at 2.2 µg/mL (Kindly provided by Prof. Leon Terstappen); and Anti-EpCAM clone Ber-EP4 at 1.9 µg/mL (Dako, Glostrup, Denmark). Staining was performed for 30 min at 37 ˚C. After washing, cells were resuspended in 100 µL of PBS with 10% AB-serum containing Phycoerythrin (PE)-conjugated Rat anti-mouse lgk light chain secondary antibody clone 187.1 at 0.01

mg/mL (BD Pharmingen, San Diego, CA, USA), and incubated for 30 min at 37 °C. After washing, cells were resuspended in PBS and PE intensity was analyzed by flow cytometry on a FACSCanto (BD Biosciences, San José, CA, USA).

4.3. Enrichment of Cells Using the IsoFlux System

The processing of samples in the IsoFlux system (Fluxion Biosciences, CA, USA) was performed according to the standard manufacturer protocol and using the low volume holder to recover samples. Three different types of beads/kits commercially available from Fluxion Biosciences were tested for enrichment in the system (Table 1); the amount and coupling of the different beads was conducted according to the respective protocols. In the absence of staining, following enrichment, the output sample from the low volume recovery holder was resuspended in 100 µL of IsoFlux binding buffer and then transferred directly unto one field of a 14 mm 3-field adhesive slide for microscopy (Erie Scientific LLC, Portsmouth, NH, USA). The holder was subsequently washed twice with 100µL of binding buffer (final volume in the slide field was 300 µL). Subsequently, 20 µL of Vectashield mounting medium (Vector Laboratories, Burlingame, CA, USA) was pipetted over the samples and the water content of the sample was allowed to evaporate overnight at room temperature, protected from the light. In case of staining, enriched cells were similarly treated, but recovered into a 1.5 mL tube and processed manually according to the protocol of the IsoFlux Circulating Tumor Cell Enumeration Kit (Fluxion). Subsequently, cells were also transferred unto a microscope slide and treated as described above. On the next day, a coverslip was applied and the samples were scanned automatically in an Eclipse E400 fluorescence microscope (Nikon, Japan), equipped with an automated XY stage controlled with home-built software, a 10x objective, a DAPI filter (Ex 377/50; Em 409/LP), a FITC filter (Ex 482/18; Em 520/28), an APC filter (Ex 640/30; Em 520/28), and a monochromatic camera. Exposure times were 10 ms for the detection of Hoechst, 200 ms for MUC-1-AF488, and 2000 ms for EpCAM-AF647.

Images were analyzed using ICY software (http://icy.bioimageanalysis.org/) and enumeration was done manually.

4.4. Enrichment of Cells Using the KingFisher Duo Prime Purification System

Different programs were designed to enrich rare cells from the mimicked-DLA product (see Figure S3) and these were used in different experiments in the present work, as indicated. Four different types of magnetic beads commercially available from Thermo Fisher Scientific were tested for enrichment in the system (Table 1).

For each bead type, we have tested three different amounts of beads (MIN, MID, and MAX) (see Table 1, Table S1, Figures S1 and S2). Coupling of the beads was conducted according to the respective manufacturer protocol, and the resulting coupled beads were resuspended in 200 µL of binding buffer (0.1% BSA, 2 mM EDTA in PBS). Beads, sample and buffers for the enrichment protocol were added to a Microtiter DeepWell 96 plate (Thermo Fisher Scientific, Dreieich, Germany) and the enrichment was executed according to the protocol scheme (See Figure S3). For the "WuDuo1S" and "WuDuo2S" protocols, the antibody mix used for staining samples was composed of AF647-conjugated anti-CD45 clone HI30 at 4 µg/mL (Biolegend, San Diego, CA, USA), AF488-conjugated anti-CK19 clone A53-B/A2 at 3.5 µg/mL (Exbio, Czech Republic), AF488-conjugated anti-panCK clone C11 at 3.5 µg/mL (Abcam, Cambridge, United Kingdom), in 1x BD Perm/wash (BD Biosciences, San Diego, CA, USA), in a total volume of 200 µL. In these two protocols, the nuclear staining solution was Hoechst 33342 (Invitrogen, Eugene, OR, USA) at 2 µg/mL, diluted in PBS. After enrichment/staining, the sample (130 µL) was transferred unto one field of a 14 mm 3-field adhesive slide for microscopy (Erie Scientific LLC, Portsmouth, NH, USA), and the sample well was further washed twice with 85 µL (the total volume in the slide field was 300 µL). The sample on the slide was treated and scanned automatically, as described above.

5. Conclusions

In conclusion, here, we demonstrate that both IsoFlux and KingFisher systems can enrich rare cells spiked in high concentrated blood samples, but the KingFisher system offers a set of user-definable features that, combined, are unique in the CTC field: the possibility of using different beads, different epitopes, automated protocols for sequential steps of enrichment, automated protocols combining enrichment and staining, and automated protocols combining depletion and positive enrichment further expand the applicability of the instrument. Furthermore, the good performance, the low costs and the

high throughput makes the system suitable for the systematic enrichment of CTCs from clinical DLA samples (Table 2).

Table 2. Resume of advantages and disadvantages found for both systems for CTC enumeration.

Isoflux	
Advantages	**Disadvantages**
• Easy to use • Some flexibility concerning the type of beads	• One single running modus • Staining is done manually
KingFisher	
Advantages	**Disadvantages**
• Easy to use • Inexpensive technology • The running protocol can be customized and it can include multiple steps for enrichment with different epitopes, depletion of CD45 cells, and subsequent staining of samples • Up to 96 samples can be run in parallel • Flexibility concerning the type of beads • Beads available combining high recovery and possibility of staining	• Reagents are not provided as a kit Any change in the running protocol requires validation • Any change in the running protocol requires validation

Supplementary Materials: The following are available online at http://www.mdpi.com/2072-6694/12/4/933/s1: Table S1: Different amounts of Thermo Fisher beads used for enrichment in the KingFisher system, Figure S1: Estimation of the size of Iso-CEK and Iso-RCEK beads, Figure S2: Determination of the concentration of the Iso-CEK beads, Figure S3: Plate setup and protocols used for enrichment of CTCs in the KingFisher instrument, Figure S4: Recovery of CAPAN-1 and HuP-T4 using the CellSearch system, Figure S5: Recovery of HuP-T4 and CAPAN-1 with four different types of beads, Figure S6: Effect of cell preservative in the recovery of CAPAN-1 cells, Figure S7: Recovery of CAPAN-1 cells spiked in whole blood samples, and recovery of colon and breast cancer cell lines spiked in mimicked-DLA products, Figure S8: Determination of the number of white blood cells co-enriched in KingFisher system using BioBMAX-VU1D9 beads, Figure S9: EpCAM-based enrichment after depletion of CD45pos cells, Figure S10: Capturing of staining antibodies by the beads.

Author Contributions: Conceptualization, N.H.S. and R.P.L.N.; methodology, J.W., A.K. and S.P.; investigation, J.W., K.R., R.G. and B.B.; resources, W.T.K. and N.H.S.; writing—original draft preparation, J.W. and R.P.L.N.; writing—review and editing, G.F. and N.H.S.; supervision, W.T.K., N.H.S. and R.P.L.N.; project administration, G.V.D.; funding acquisition, W.T.K. and N.H.S. All authors have read and agreed to the published version of the manuscript.

Funding: This research was funded by the Brigitte und Dr. Konstanze Wegener Foundation, Project #01 to N.H.S. and W.T.K.; and the Innovative Medicines Initiative Joint Undertaking (IMI JU) in conjunction with CANCER-ID, Grant Agreement #115749 to N.H.S.

Conflicts of Interest: The KingFisher Instrument used in the research reported in this paper was loaned to the University Hospital and Medical Faculty of the Heinrich-Heine University Dusseldorf, by Thermo Fisher Scientific, Inc., free of charge. All KingFisher consumables used in the research reported in this paper were provided to University Hospital and Medical Faculty of the Heinrich-Heine University Dusseldorf, free of charge. Suraj Patel and Andreas Koch are employees of Thermo Fisher Scientific, Inc. All the other authors have declared no potential conflict of interests. The funders had no role in the design of the study; in the collection, analyses, or interpretation of data; in the writing of the manuscript, or in the decision to publish the results.

References

1. Wang, H.; Stoecklein, N.H.; Lin, P.P.; Gires, O. Circulating and disseminated tumor cells: Diagnostic tools and therapeutic targets in motion. *Oncotarget* **2017**, *8*, 1884–1912. [CrossRef] [PubMed]
2. Pantel, K.; Speicher, M.R. The biology of circulating tumor cells. *Oncogene* **2015**, *35*, 1216–1224. [CrossRef] [PubMed]
3. Alix-Panabieres, C.; Pantel, K. Challenges in circulating tumour cell research. *Nat. Rev. Cancer* **2014**, *14*, 623–631. [CrossRef] [PubMed]
4. Stoecklein, N.H.; Fischer, J.C.; Niederacher, D.; Terstappen, L.W. Challenges for ctc-based liquid biopsies: Low CTC frequency and diagnostic leukapheresis as a potential solution. *Expert Rev. Mol. Diagn.* **2016**, *16*, 147–164. [CrossRef] [PubMed]
5. Tibbe, A.G.; Miller, M.C.; Terstappen, L.W. Statistical considerations for enumeration of circulating tumor cells. *Cytom. Part A J. Int. Soc. Anal. Cytol.* **2007**, *71*, 154–162. [CrossRef] [PubMed]
6. Fischer, J.C.; Niederacher, D.; Topp, S.A.; Honisch, E.; Schumacher, S.; Schmitz, N.; Zacarias Fohrding, L.; Vay, C.; Hoffmann, I.; Kasprowicz, N.S.; et al. Diagnostic leukapheresis enables reliable detection of circulating tumor cells of nonmetastatic cancer patients. *Proc. Natl. Acad. Sci. USA* **2013**, *110*, 16580–16585. [CrossRef]
7. Andree, K.C.; Mentink, A.; Zeune, L.L.; Terstappen, L.; Stoecklein, N.H.; Neves, R.P.; Driemel, C.; Lampignano, R.; Yang, L.; Neubauer, H.; et al. Towards a real liquid biopsy in metastatic breast and prostate cancer: Diagnostic leukapheresis increases ctc yields in a european prospective multi-center study (ctctrap). *Int. J. Cancer. J. Int. Du Cancer* **2018**, *143*, 2584–2591. [CrossRef]
8. Lambros, M.B.; Seed, G.; Sumanasuriya, S.; Gil, V.; Crespo, M.; Fontes, M.S.; Chandler, R.; Mehra, N.; Fowler, G.; Ebbs, B.; et al. Single cell analyses of prostate cancer liquid biopsies acquired by apheresis. *Clin. Cancer Res. Off. J. Am. Assoc. Cancer Res.* **2018**, *24*, 5635–5644. [CrossRef]
9. Fehm, T.N.; Meier-Stiegen, F.; Driemel, C.; Jager, B.; Reinhardt, F.; Naskou, J.; Franken, A.; Neubauer, H.; Neves, R.P.L.; van Dalum, G.; et al. Diagnostic leukapheresis for ctc analysis in breast cancer patients: Ctc frequency, clinical experiences and recommendations for standardized reporting. *Cytom. Part A J. Int. Soc. Anal. Cytol.* **2018**, *93*, 1213–1219. [CrossRef]
10. Gires, O.; Stoecklein, N.H. Dynamic epcam expression on circulating and disseminating tumor cells: Causes and consequences. *Cell. Mol. Life Sci.* **2014**, *71*, 4393–4402. [CrossRef]
11. Krebs, M.G.; Metcalf, R.L.; Carter, L.; Brady, G.; Blackhall, F.H.; Dive, C. Molecular analysis of circulating tumour cells-biology and biomarkers. *Nat. Rev. Clin. Oncol.* **2014**, *11*, 129–144. [CrossRef] [PubMed]
12. Allard, W.J.; Terstappen, L.W. Ccr 20th anniversary commentary: Paving the way for circulating tumor cells. *Clin. Cancer Res. Off. J. Am. Assoc. Cancer Res.* **2015**, *21*, 2883–2885. [CrossRef] [PubMed]
13. Allard, W.J.; Matera, J.; Miller, M.C.; Repollet, M.; Connelly, M.C.; Rao, C.; Tibbe, A.G.; Uhr, J.W.; Terstappen, L.W. Tumor cells circulate in the peripheral blood of all major carcinomas but not in healthy subjects or patients with nonmalignant diseases. *Clin. Cancer Res. Off. J. Am. Assoc. Cancer Res.* **2004**, *10*, 6897–6904. [CrossRef] [PubMed]
14. Swennenhuis, J.F.; van Dalum, G.; Zeune, L.L.; Terstappen, L.W. Improving the cellsearch(r) system. *Expert Rev. Mol. Diagn.* **2016**, *16*, 1291–1305. [CrossRef] [PubMed]
15. Harb, W.; Fan, A.; Tran, T.; Danila, D.C.; Keys, D.; Schwartz, M.; Ionescu-Zanetti, C. Mutational analysis of circulating tumor cells using a novel microfluidic collection device and qpcr assay. *Transl. Oncol.* **2013**, *6*, 528–538. [CrossRef]
16. Tseng, H.C.; Lee, A.W.; Wei, P.L.; Chang, Y.J. Clinical diagnosis of colorectal cancer using electrospun triple-blend fibrous mat-based capture assay of circulating tumor cells. *J. Mater. Chem. B* **2016**, *4*, 6565–6580. [CrossRef]
17. Xu, L.; Mao, X.; Imrali, A.; Syed, F.; Mutsvangwa, K.; Berney, D.; Cathcart, P.; Hines, J.; Shamash, J.; Lu, Y.J. Optimization and evaluation of a novel size based circulating tumor cell isolation system. *PLoS ONE* **2015**, *10*, e0138032. [CrossRef]
18. Sanchez-Lorencio, M.I.; Ramirez, P.; Saenz, L.; Martinez Sanchez, M.V.; De La Orden, V.; Mediero-Valeros, B.; Veganzones-De-Castro, S.; Baroja-Mazo, A.; Revilla Nuin, B.; Gonzalez, M.R.; et al. Comparison of two types of liquid biopsies in patients with hepatocellular carcinoma awaiting orthotopic liver transplantation. *Transplant. Proc.* **2015**, *47*, 2639–2642. [CrossRef]

19. Alva, A.; Friedlander, T.; Clark, M.; Huebner, T.; Daignault, S.; Hussain, M.; Lee, C.; Hafez, K.; Hollenbeck, B.;
Weizer, A.; et al. Circulating tumor cells as potential biomarkers in bladder cancer. *J. Urol.* **2015**, *194*, 790–798. [CrossRef]
20. Yang, G.; Erdman, D.E.; Kodani, M.; Kools, J.; Bowen, M.D.; Fields, B.S. Comparison of commercial systems for extraction of nucleic acids from DNA/rna respiratory pathogens. *J. Virol. Methods* **2011**, *171*, 195–199. [CrossRef]
21. Arola, H.O.; Tullila, A.; Kiljunen, H.; Campbell, K.; Siitari, H.; Nevanen, T.K. Specific noncompetitive immunoassay for ht-2 mycotoxin detection. *Anal. Chem.* **2016**, *88*, 2446–2452. [CrossRef] [PubMed]
22. Khoja, L.; Backen, A.; Sloane, R.; Menasce, L.; Ryder, D.; Krebs, M.; Board, R.; Clack, G.; Hughes, A.; Blackhall, F.; et al. A pilot study to explore circulating tumour cells in pancreatic cancer as a novel biomarker. *Br. J. Cancer* **2012**, *106*, 508–516. [CrossRef]
23. Akita, H.; Nagano, H.; Takeda, Y.; Eguchi, H.; Wada, H.; Kobayashi, S.; Marubashi, S.; Tanemura, M.; Takahashi, H.; Ohigashi, H.; et al. Ep-cam is a significant prognostic factor in pancreatic cancer patients by suppressing cell activity. *Oncogene* **2011**, *30*, 3468–3476. [CrossRef] [PubMed]
24. Fong, D.; Steurer, M.; Obrist, P.; Barbieri, V.; Margreiter, R.; Amberger, A.; Laimer, K.; Gastl, G.; Tzankov, A.; Spizzo, G. Ep-cam expression in pancreatic and ampullary carcinomas: Frequency and prognostic relevance. *J. Clin. Pathol.* **2008**, *61*, 31–35. [CrossRef]
25. Bidard, F.C.; Huguet, F.; Louvet, C.; Mineur, L.; Bouche, O.; Chibaudel, B.; Artru, P.; Desseigne, F.; Bachet, J.B.;
Mathiot, C.; et al. Circulating tumor cells in locally advanced pancreatic adenocarcinoma: The ancillary circe 07 study to the lap 07 trial. *Ann. Oncol. Off. J. Eur. Soc. Med. Oncol./ESMO* **2013**, *24*, 2057–2061. [CrossRef] [PubMed]
26. Kurihara, T.; Itoi, T.; Sofuni, A.; Itokawa, F.; Tsuchiya, T.; Tsuji, S.; Ishii, K.; Ikeuchi, N.; Tsuchida, A.; Kasuya, K.; et al. Detection of circulating tumor cells in patients with pancreatic cancer: A preliminary result. *J. Hepato-Biliary-Pancreat. Surg.* **2008**, *15*, 189–195. [CrossRef]
27. Earl, J.; Garcia-Nieto, S.; Martinez-Avila, J.C.; Montans, J.; Sanjuanbenito, A.; Rodriguez-Garrote, M.; Lisa, E.; Mendia, E.; Lobo, E.; Malats, N.; et al. Circulating tumor cells (CTC) and KRAS mutant circulating free dna (CFDNA) detection in peripheral blood as biomarkers in patients diagnosed with exocrine pancreatic cancer. *BMC Cancer* **2015**, *15*, 797. [CrossRef]
28. Brychta, N.; Drosch, M.; Driemel, C.; Fischer, J.C.; Neves, R.P.; Esposito, I.; Knoefel, W.; Mohlendick, B.; Hille, C.; Stresemann, A.; et al. Isolation of circulating tumor cells from pancreatic cancer by automated filtration. *Oncotarget* **2017**, *8*, 86143–86156. [CrossRef]
29. Qu, C.F.; Li, Y.; Song, Y.J.; Rizvi, S.M.; Raja, C.; Zhang, D.; Samra, J.; Smith, R.; Perkins, A.C.; Apostolidis, C.; et al. Muc1 expression in primary and metastatic pancreatic cancer cells for in vitro treatment by (213)bi-c595 radioimmunoconjugate. *Br. J. Cancer* **2004**, *91*, 2086–2093. [CrossRef]
30. Li, Y.; Cozzi, P.J. Muc1 is a promising therapeutic target for prostate cancer therapy. *Curr. Cancer Drug Targets* **2007**, *7*, 259–271. [CrossRef]
31. Gold, D.V.; Cardillo, T.; Goldenberg, D.M.; Sharkey, R.M. Localization of pancreatic cancer with radiolabeled monoclonal antibody pam4. *Crit. Rev. Oncol./Hematol.* **2001**, *39*, 147–154. [CrossRef]
32. Dotan, E.; Alpaugh, R.K.; Ruth, K.; Negin, B.P.; Denlinger, C.S.; Hall, M.J.; Astsaturov, I.; McAleer, C.; Fittipaldi, P.; Thrash-Bingham, C.; et al. Prognostic significance of muc-1 in circulating tumor cells in patients with metastatic pancreatic adenocarcinoma. *Pancreas* **2016**, *45*, 1131–1135. [CrossRef] [PubMed]
33. Thege, F.I.; Lannin, T.B.; Saha, T.N.; Tsai, S.; Kochman, M.L.; Hollingsworth, M.A.; Rhim, A.D.; Kirby, B.J. Microfluidic immunocapture of circulating pancreatic cells using parallel epcam and muc1 capture: Characterization, optimization and downstream analysis. *Lab Chip* **2014**, *14*, 1775–1784. [CrossRef] [PubMed]
34. Chebouti, I.; Kasimir-Bauer, S.; Buderath, P.; Wimberger, P.; Hauch, S.; Kimmig, R.; Kuhlmann, J.D. Emt-like circulating tumor cells in ovarian cancer patients are enriched by platinum-based chemotherapy. *Oncotarget* **2017**, *8*, 48820–48831. [CrossRef]

35. Blassl, C.; Kuhlmann, J.D.; Webers, A.; Wimberger, P.; Fehm, T.; Neubauer, H. Gene expression profiling of single circulating tumor cells in ovarian cancer-establishment of a multi-marker gene panel. *Mol. Oncol.* **2016**, *10*, 1030–1042. [CrossRef] [PubMed]
36. Aktas, B.; Kasimir-Bauer, S.; Muller, V.; Janni, W.; Fehm, T.; Wallwiener, D.; Pantel, K.; Tewes, M.; Group, D.S. Comparison of the her2, estrogen and progesterone receptor expression profile of primary tumor, metastases and circulating tumor cells in metastatic breast cancer patients. *BMC Cancer* **2016**, *16*, 522. [CrossRef]
37. Guglielmi, R.; Lai, Z.; Raba, K.; van Dalum, G.; Behrens, B.; Bhagat, A.A.S.; Knoefel, W.T.; Neves, R.P.L.; Stoecklein, N.H. A label-free enrichment method to isolate CTCs from larger blood volumes and diagnostic leukapheresis products. *Sci. Rep.* **2020**. Under review.
38. Lai, C.H.; Tsai, W.S.; Yang, M.H.; Chou, T.Y.; Chang, Y.C. A two-dimensional immunomagnetic nano-net for the efficient isolation of circulating tumor cells in whole blood. *Nanoscale* **2019**, *11*, 21119–21127. [CrossRef]
39. Lai, C.H.; Choon Lim, S.; Wu, L.C.; Wang, C.F.; Tsai, W.S.; Wu, H.C.; Chang, Y.C. Site-specific antibody modification and immobilization on a microfluidic chip to promote the capture of circulating tumor cells and microemboli. *Chem. Commun. (Cambridge)* **2017**, *53*, 4152–4155. [CrossRef]
40. Makaraviciute, A.; Ramanaviciene, A. Site-directed antibody immobilization techniques for immunosensors. *Biosens. Bioelectron.* **2013**, *50*, 460–471. [CrossRef]
41. Schasfoort, R.B.; Andree, K.C.; van der Velde, N.; van der Kooi, A.; Stojanovic, I.; Terstappen, L.W. Interpolation method for accurate affinity ranking of arrayed ligand-analyte interactions. *Anal. Biochem.* **2016**, *500*, 21–23. [CrossRef] [PubMed]
42. Kuo, S.C.; Lauffenburger, D.A. Relationship between receptor/ligand binding affinity and adhesion strength. *Biophys. J.* **1993**, *65*, 2191–2200. [CrossRef]
43. Neuhaus, E.M.; Horstmann, H.; Almers, W.; Maniak, M.; Soldati, T. Ethane-freezing/methanol-fixation of cell monolayers: A procedure for improved preservation of structure and antigenicity for light and electron microscopies. *J. Struct. Biol.* **1998**, *121*, 326–342. [CrossRef] [PubMed]
44. Melan, M.A. Overview of cell fixation and permeabilization. *Methods Mol. Biol.* **1994**, *34*, 55–66.
45. Chantima, W.; Thepthai, C.; Cheunsuchon, P.; Dharakul, T. Epcam expression in squamous cell carcinoma of the uterine cervix detected by monoclonal antibody to the membrane-proximal part of epcam. *BMC Cancer* **2017**, *17*, 811. [CrossRef]
46. De Albuquerque, A.; Kubisch, I.; Breier, G.; Stamminger, G.; Fersis, N.; Eichler, A.; Kaul, S.; Stolzel, U. Multimarker gene analysis of circulating tumor cells in pancreatic cancer patients: A feasibility study. *Oncology* **2012**, *82*, 3–10. [CrossRef]
47. Demel, U.; Tilz, G.P.; Foeldes-Papp, Z.; Gutierrez, B.; Albert, W.H.; Bocher, O. Detection of tumour cells in the peripheral blood of patients with breast cancer. Development of a new sensitive and specific immunomolecular assay. *J. Exp. Clin. Cancer Res.* **2004**, *23*, 465–468.
48. Hauch, S.; Zimmermann, S.; Lankiewicz, S.; Zieglschmid, V.; Bocher, O.; Albert, W.H. The clinical significance of circulating tumour cells in breast cancer and colorectal cancer patients. *Anticancer Res.* **2007**, *27*, 1337–1341. 49. Agerbaek, M.O.; Bang-Christensen, S.R.; Yang, M.H.; Clausen, T.M.; Pereira, M.A.; Sharma, S.; Ditlev, S.B.; Nielsen, M.A.; Choudhary, S.; Gustavsson, T.; et al. The var2csa malaria protein efficiently retrieves circulating tumor cells in an epcam-independent manner. *Nat. Commun.* **2018**, *9*, 3279. [CrossRef]
50. Pezzi, H.M.; Niles, D.J.; Schehr, J.L.; Beebe, D.J.; Lang, J.M. Integration of magnetic bead-based cell selection into complex isolations. *ACS Omega* **2018**, *3*, 3908–3917. [CrossRef]

Supplementary Materials:

Magnetic-Based Enrichment of Rare Cells from High Concentrated Blood Samples

Junhao Wu, Katharina Raba, Rosa Guglielmi, Bianca Behrens, Guus Van Dalum, Georg Flügen, Andreas Koch, Suraj Patel, Wolfram T. Knoefel, Nikolas H. Stoecklein and Rui P. L. Neves

Table 1. Different amounts of Thermo Fisher beads used for enrichment in the KingFisher system

Amount	Total surface area	Type of Beads							
		Dy-EpE		Dy-ACK		Dy-BioB		Pi-Biot	
		Number of beads	Volume from original bead suspension	Number of beads	Volume from original bead suspension	Number of beads	Volume from original bead suspension	Number of beads	Volume from original bead suspension
Minimal (MIN)	6.1×10^7 μm²	9.6×10^5	2.4 μL	24.8×10^5	3.7 μL	24.8×10^5	6.2 μL	191.5×10^5	2.0 μL
Middle (MID)	5× MIN = 30.6×10^7 μm²	19.2×10^5	12.0 μL	124×10^5	18.5 μL	124×10^5	31.0 μL	957.7×10^5	10.0 μL
Maximal (MAX)	10 × MIN = 61.1×10^7 μm²	38.4×10^5	24.0μL	248×10^5	37.0 μL	248×10^5	62.0 μL	1915.4×10^5	19.9 μL

Notes: The minimal (MIN) surface area is equivalent to the total surface area provided by the Iso-CEK beads in a standard IsoFlux CTC Enrichment Kit assay, which was calculated upon determination of the size (Figure S2) and number (Figure S3) of Iso-CEK beads used in an IsoFlux CTC Enrichment Kit assay. Middle surface area (MID) was subsequently defined as 5xMIN, and the maximal surface area (MAX) was defined as 10xMIN.

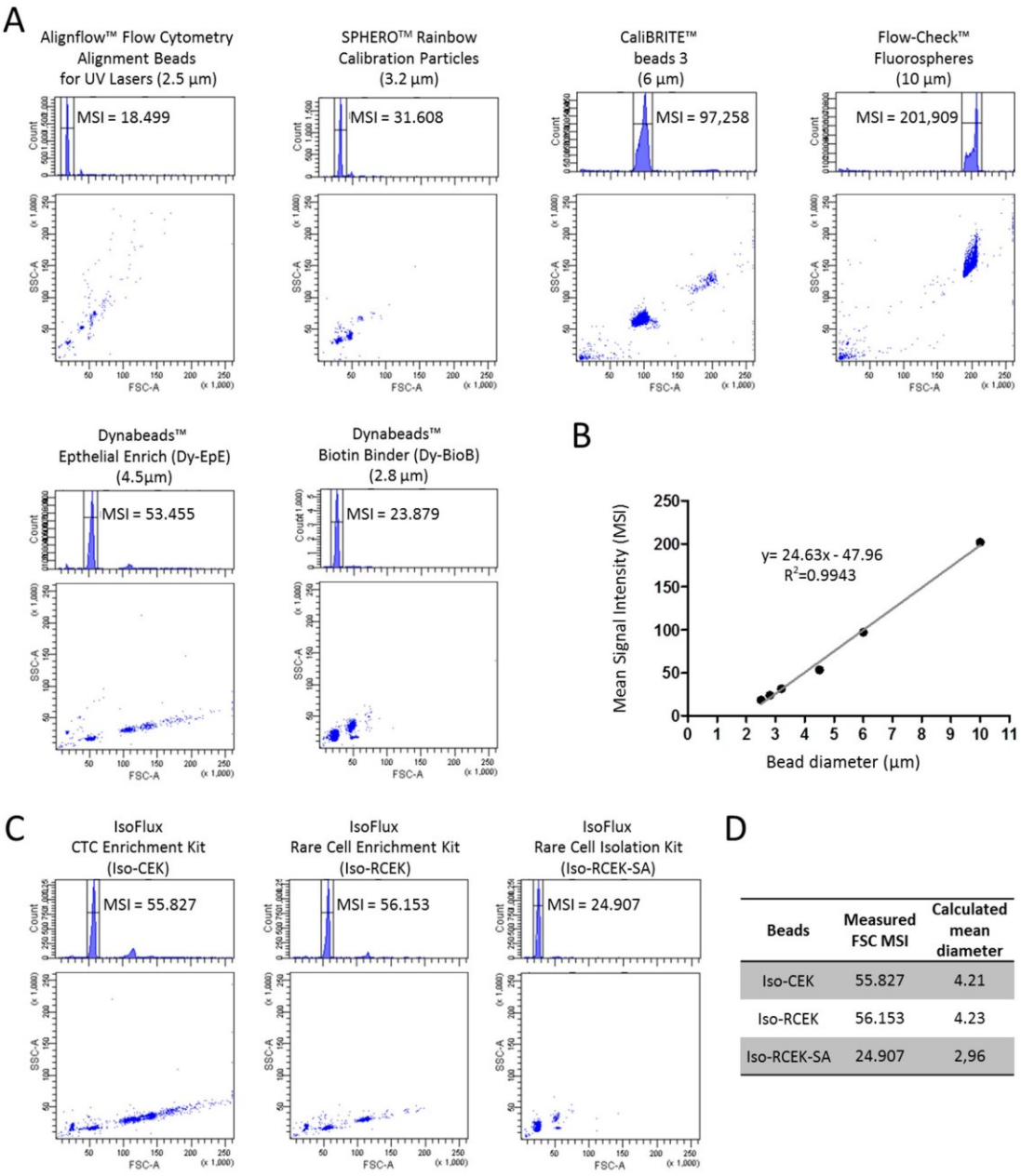

Beads	Measured FSC MSI	Calculated mean diameter
Iso-CEK	55.827	4.21
Iso-RCEK	56.153	4.23
Iso-RCEK-SA	24.907	2,96

Figure S1. Estimation of the size of Iso-CEK, Iso-RCEK and Iso-RECK-SA beads. **(A)** Forward (FSC) and Side Scatter (SSC) dot plots and Forward scatter (FCS) histograms obtained by flow cytometry in a FACSCanto (BD) (SSC at a voltage of 346 V and FSC at 220 V) for six beads with known sizes: (i) Alignflow Flow Cytometry Alignment Beads for UV Lasers (Molecular Probes, Oregon, USA, #A16502) with 2.5 µm; (ii) SPHERO Rainbow Calibration Particles (Spherotech, #RCP-30-5A-2) with 3.2 µm; (iii) CaliBRITE beads 3 (BD, #340486) with 6 µm; (iv) Flow-Check Fluorospheres (Beckman Coulter, CA, USA, #6605359), with 10 µm; (v) Dy-EpE with 4.5 µm; (vi) Dy-BioB with 2.8 µm. For each type of bead the mean signal intensity (MSI) of the single bead population depicted in the histograms was determined. **(B)** Linear regression calculated from the correlation between diameter and FSC- MSI of the beads in (A). **(C)** Flow cytometry analysis of the Iso-CEK, Iso-RCEK, and Iso-RCEK-SA beads as done in (A). **(D)** Calculation of approximate bead diameter using the equation of the linear regression established in (B).

A

Dilution from original Dy-EpE bead suspension ($4x10^8$/ml)	Dy-EpE bead concentration ($x10^8$/ml)	Measured OD600
1:15	0.266667	28.415
1:16	0.250000	28.676
1:17	0.235294	28.207
1:20	0.200000	21.057
1:25	0.160000	19.560
1:30	0.133333	13.999
1:35	0.114286	12.442
1:40	0.100000	11.495
1:45	0.088889	10.174

B

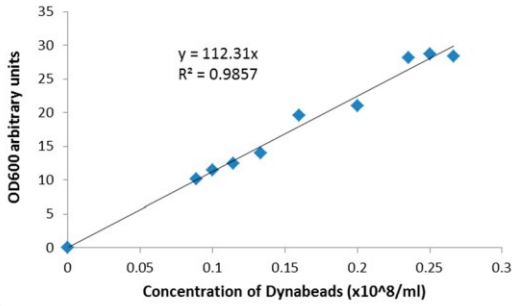

C

Dilution from Iso-CEK bead suspension	Measured OD600	Calculated Iso-CEK bead concentration in the original suspension ((OD600/112.31)*dilution)
1:1	27.404	0.244 $x10^8$/ml
1:2	16,060	0.286 $x10^8$/ml
1:4	8,171	0.291 $x10^8$/ml
	Mean:	0.274 $x10^8$/ml

D

Calculated concentration of Iso-CEK beads in the original bead suspension (C)	0.274 $x10^8$/ml
Volume of bead suspension used per sample in the IsoFlux CTC Enrichment Kit according to protocol (V)	40 µl
Calculated number of beads used per sample in the IsoFlux CTC Enrichment Kit assay (N=C*V)	10.96 $x10^5$ beads
Calculated concentration of beads used per sample (N/V)	10.96 $x10^5$/ml
Calculated diameter of Iso-CEK beads (from SupplementalFigure 2)	4,2143 µm
Surface area of a single bead ($A = 4\pi r^2$)	55.79 μm^2
Total surface area available for interaction with cells in IsoFlux CTC Enrichment Kit assay (Total Area=N*A)	6.11 $x10^7$ μm^2

Figure S2. Determination of the concentration of the Iso-CEK beads and the surface area of Iso-CEK beads available for interaction with cells in the IsoFlux CTC Enrichment Kit assay. The concentration of Iso-CEK beads was determined by comparing the optical density at 600 nm (OD600) of Iso-CEK bead suspensions with that of Dynabeads Epithelial Enrich (Thermo Fisher Scientific, #16102) bead suspensions with similar nominal size. (A) OD600 of a series of dilutions from the original Dy-EpE bead suspension at 4x108 beads/ml. OD600 was measured in a BioPhotometer (Eppendorf, Germany) using disposable cuvettes (Sarstedt, Germany). (B) Standard curve made with the measurements in (A). (C) OD600 of a three dilutions from the original Iso-CEK bead suspension and the concentration of Iso-CEK beads in the original suspension calculated based on the formula of the standard curve obtained in (B). OD600 was measured as in (A). (D) Parameters and steps used to calculate the total surface area of the beads that is available for interaction with cells in a standard IsoFlux CTC Enrichment Kit assay where Iso-CEK beads are employed.

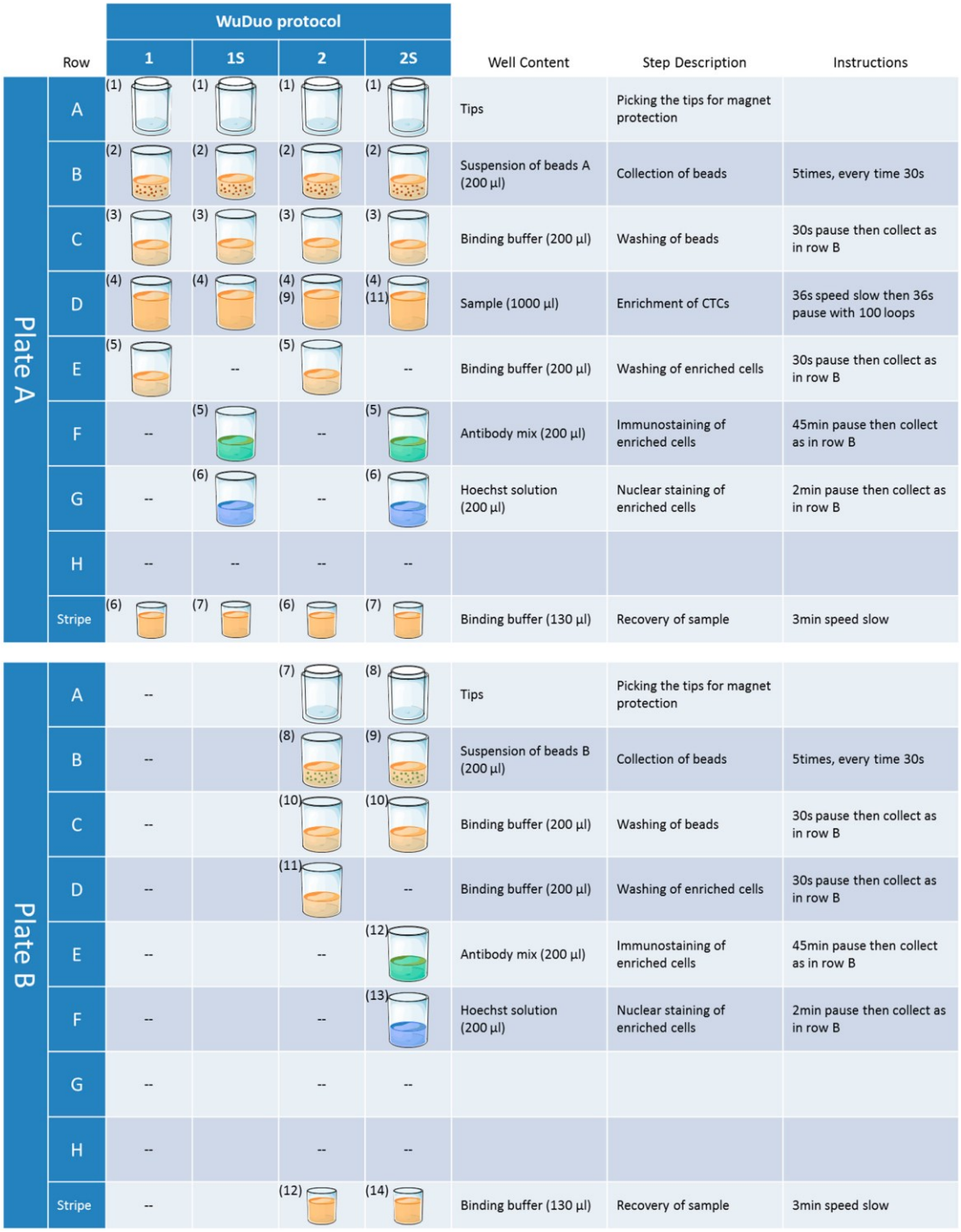

Figure S3. Plate setup and protocols used for enrichment of CTCs in the KingFisher instrument. Illustration of the 4 WuDuo protocols (WuDuo 1, 1S, 2 and 2S) including the content of the plate, description of each step and the KingFisher settings. The sequence of the steps in the respective protocol (each row) is indicated by the number (n) next to the illustration of each well. The cups items used in this figure were extracted from "Medical Equipment" attributed to Servier Medical Art. These were used and adapted under a Creative Commons Attribution 3.0 Unported License.

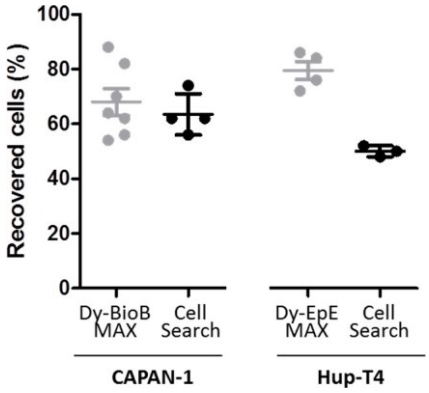

Figure S4. Recovery of CAPAN-1 and HuP-T4 using the CellSearch system. One day prior to the experiment, 1x108 PBMNCs were resuspended in 8 mL of PBS containing 0.1% BSA and 2 mM EDTA, transferred into a CellSave preservative tube (Menarini Silicon Biosystems, Huntingdon Valley, PA, USA), and incubated overnight at room temperature on a rotator. Separately, CAPAN-1 or HuP-T4 cells harvested from culture were treated similarly. On the next day, 50 cell line cells were spiked by flow cytometry into the CellSave tube containing the PBMNCs, enriched with the CellSearch CTC Kit in the CellTrack Autoprep (Menarini Silicon Biosystems, San Diego, CA, USA), and enumerated in the CellTrack Analyzer II (Menarini Silicon Biosystems) according to the manufacturer standard procedure. Recovery data from cells with Dy-BioB and Dy-EpE beads (in gray in the graph) is the same as in Figure 1 of the main manuscript.

A

		Hup-T4					CAPAN-1				
	Cells spiked	1	10	30	50	100	1	10	30	50	100
Cells recovered	Iso-CEK	1	3	13	19	56	0	5	15	30	37
		1	6	19	18	51	1	4	14	23	43
		1	4	21	28	62	1	4	6	20	42
					35					17	
					25					25	
					36						
	Iso-RCEK (BerEP4)	1	5	18	31	53	1	6	9	25	26
		1	2	15	22	49	1	3	13	14	31
		1	3	14	19	36	1	2	11	21	43
					23					19	
					31					21	
	Dy-EpE^{MID}	1	6	18	37	80	0	3	17	31	52
		1	4	22	37	78	0	5	12	38	47
		1	9	17	41	74	1	5	13	23	48
					35					28	
	Dy-BioB^{MAX} (VU1D9)		6	14	34	52		2	11	27	49
			6	24	31	45		4	18	44	50
			8	19	30	42		5	12	35	49
					36					41	
										32	
										28	
										31	

B

Hup-T4

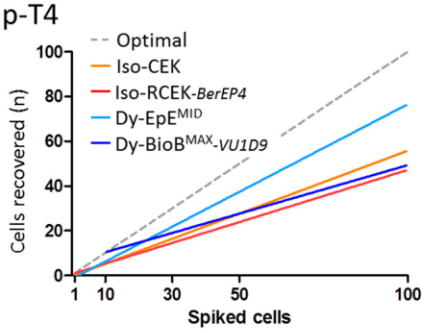

	R^2	Slope	Recovery
Optimal	1.000	1.000 ± 0.0	
Iso-CEK	0.9360	0.5615 ± 0.03672	56 %
Iso-RCEK	0.9276	0.4659 ± 0.03361	47 %
Dy-EpE	0.9913	0.7817 ± 0.01956	78 %
Dy-BioB	0.8938	0.4326 ± 0.04497	43 %

Capan-1

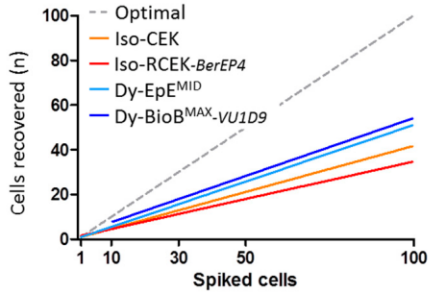

	R^2	Slope	Recovery
Optimal	1.000	1.000 ± 0.0	
Iso-CEK	0.9427	0.4120 ± 0.02622	42 %
Iso-RCEK	0.8896	0.3353 ± 0.03051	34 %
Dy-EpE	0.9513	0.5076 ± 0.03070	51 %
Dy-BioB	0.8411	0.5178 ± 0.06016	52 %

Figure S5. Recovery of HuP-T4 and CAPAN-1 with four different types of beads. One, ten, 30, 50, and 100 HuP-T4 or CAPAN-1 cells pre-labelled with CellTracker Green CMFDA Dye (Thermo Fisher Scientific) were spiked in pseudo DLA products. Enrichment was done with Iso-CEK and Iso-RCEK- BerEP4 in the IsoFlux system and with Dy-EpE and Dy-BioBMAX-VU1D9 in the KingFisher system. (A) Number of cells recovered in each experimental replicate. (B) Linear regression of the data listed in (A) with information on the linearity (R2) and slope. Recovery along the range of experiments was determined from the slope (Recovery = Slope × 100).

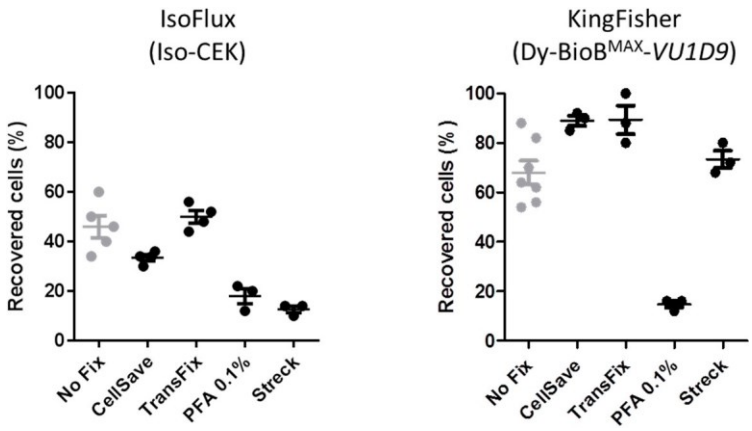

Figure S6. Effect of cell preservative in the recovery of CAPAN-1 cells. 1× 108 PBMNCs resuspended in 8 mL of PBS containing 0.1% BSA and 2 mM EDTA were transferred into CellSave preservative tube (Menarini Silicon Biosystems, Huntingdon Valley, PA, USA), TransFix Vacuum tube (ref. TVT- 09-50-45, Cytomark, Buckingham, UK), Cell-Free DNA BCT CE tube (Streck, La Vista, NE, USA) or a 15 mL conical centrifuge tube (Greiner bio-one, DE) containing 500 µL of 1.6% Paraformaldehyde (PFA) (final PFA concentration 0.1%). Tubes were incubated overnight at room temperature on a rotator. Separately, cell line cells were resuspended in 8 mL of PBS containing 0.1% BSA and 2 mM EDTA and treated similarly. On the next day, the PBMNCs samples were pelleted upon centrifugation at 400 g for 7 min, the volume of the sample was adjusted to 850 µL with PBS containing 0.1% BSA and 2 mM EDTA, and cell line cells were spiked by flow cytometry. Spiked samples were then analyzed in the IsoFlux system using the Iso-CEK beads or KingFisher system using the Dy-BioB- VU1D9 beads. Recovery data from cells without fixation (in gray in the graph) is the same as in Figure 1 of the main manuscript.

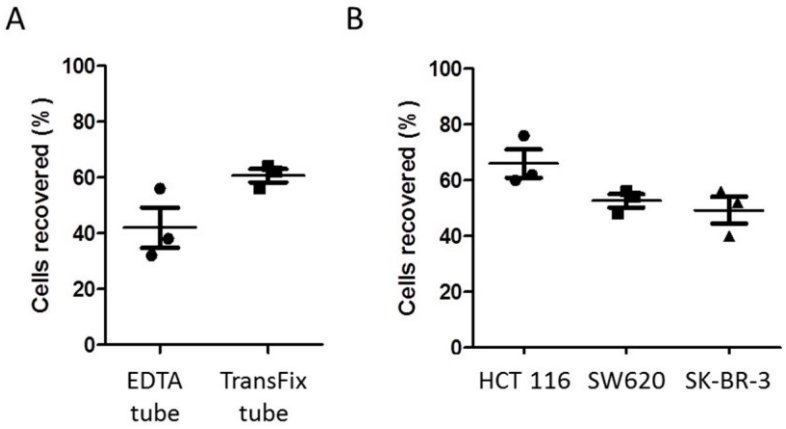

Figure S7. Recovery of CAPAN-1 cells spiked in whole blood samples, and recovery of colon and breast cancer cell lines spiked in pseudo DLA products. (A) Recovery of CAPAN-1 cells spiked in whole blood samples. 7.5 mL peripheral blood from healthy donors and collected in EDTA or TransFix tubes was treated with Red Blood Cell Lysis buffer (G-Biosciences, MO, USA) (22.5 mL and 30 mL, respectively) for 10 min at room temperature in rotation. Subsequently samples were centrifuged at 500 g for 10 min at room temperature, the supernatant was discarded, and the pellet was resuspended in 850 µL of binding buffer (0.1% BSA, 2 mM EDTA in PBS) and finally transferred into a Microtiter DeepWell 96 plate (Thermo Fisher Scientific, Germany). 50 CAPAN-1 cells pre- labelled with CellTracker Green CMFDA Dye were spiked by flow cytometry using the MoFlo XDP flow cytometer (Beckman Coulter, Krefeld, Germany) into the samples. Enrichment in the KingFisher system was executed according the WuDuo1 protocol. (B) Recovery of colon and breast cancer cell lines spiked in pseudo DLA products. 50 HCT 116, SW620 and SK-BR-3 cells pre-labelled with CellTracker Green CMFDA Dye were spiked by flow cytometry into pseudo DLA products prepared as described in the main manuscript.

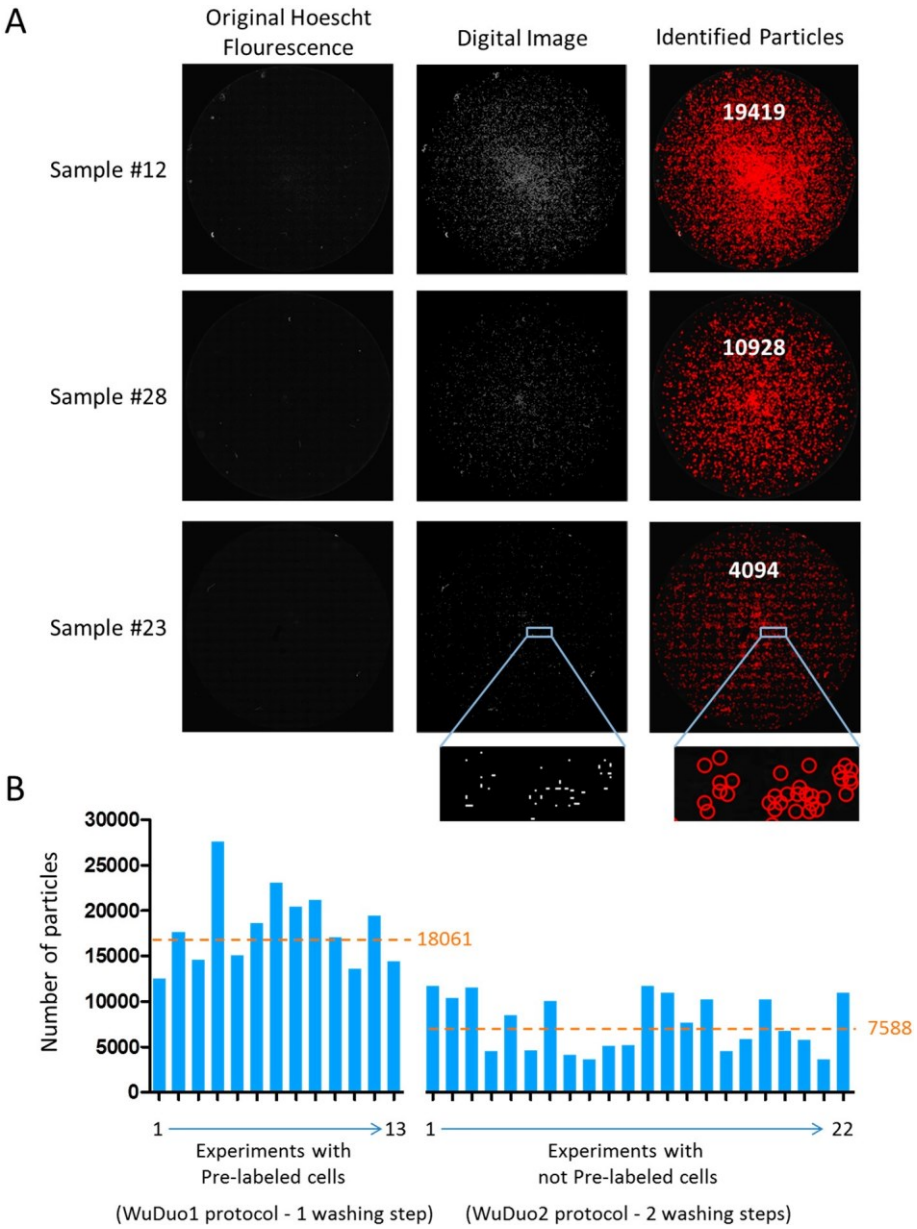

Figure S8. Determination of the number of white blood cells co-enriched in KingFisher system using BioBMAX-VU1D9 beads. To determine the total number of WBCs carried, we marked all enriched cells with Hoechst nuclear dye, making possible their subsequent identification and enumeration by fluorescence microscopy. For the staining we added Hoechst 33342 (Invitrogen, OR, USA) at 2 µg/mL to the binding buffer in well E of the WuDuo1 protocol or well G of WuDuo1S protocol. After enrichment, the sample was processed as described in the main section of the manuscript and the enriched samples were analysed by fluorescence microscopy. The images obtained were subsequently analysed with ICY software (http://www.icy.bioimageanalysis.org/) and the number of Hoechst positive cells was determined using spot detector plugin of ICY. (A) Overview montage of all images obtained from Hoescht flourescence in three representative samples. The different panels show the original fluorescence image (left), the digital image after processing with ICY software (middle), and then particles detected by the spot detector plugin (right). (B) Number of particles detected in experiments performed with the WuDuo1 and WuDuo1S protocols. The mean values are indicated and represented by the dashed lines.

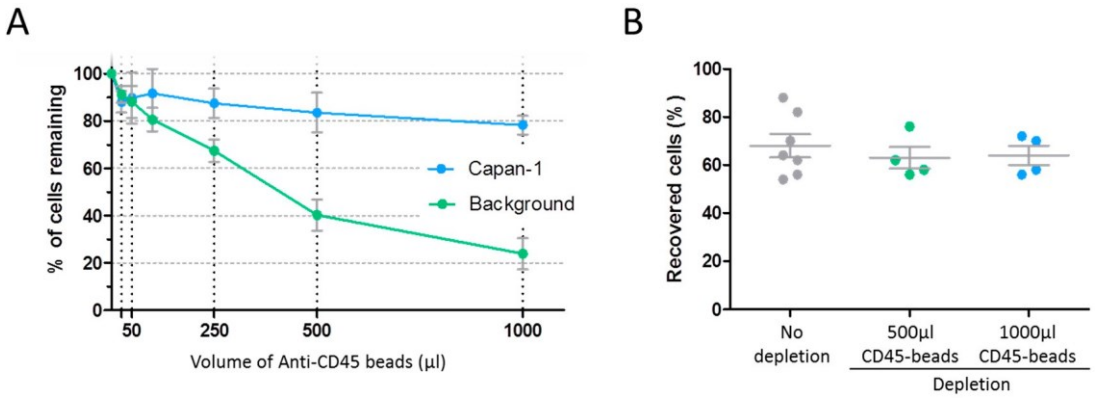

Figure S9. EpCAM-based enrichment after depletion of CD45pos cells. (A) 1 × 105 CAPAN-1 cells pre-labeled with CellTracker Green CMFDA Dye in suspension were spiked into pseudo DLA products (1 mL at 1 × 108 MNCs/mL). CD45 Depletion was performed in the KingFisher system using different volumes of Dynabeads CD45 magnetic bead suspension (Life Technologies by Thermo Fisher Scientific, Vilnius, Lithuania). After depletion, the volume of the sample was adjusted to 1 mL with binding buffer, mixed with 50 µL of CountBright absolute counting beads (0.52 × 105 beads/50 µL) (Invitrogen by Thermo Fisher Scientific, Eugene, OR, USA) and analyzed by flow cytometry in a FACSCanto (BD Biosciences, San José, CA, USA). Acquisition was stopped when 2600 or 5200 beads (5% or 10% of the sample) were detected. The number of CellTracker Green positive events (spiked cells) and CellTracker Green negative events (WBCs) was determined. In order to calculate the faction depletion (percentage as plotted), the number of cells of the two populations was correlated with the respective populations in samples where no CD45 beads were used (control). (B) Recovery of CAPAN-1 cells pre-labeled with CellTracker Green CMFDA Dye after CD45 depletion and subsequent EpCAM enrichment. 500 µL and 1000 µL Dynabeads CD45 magnetic beads were used for depletion. In gray, for comparison, is the same data as in Figure 1 of the main manuscript obtained without depletion.

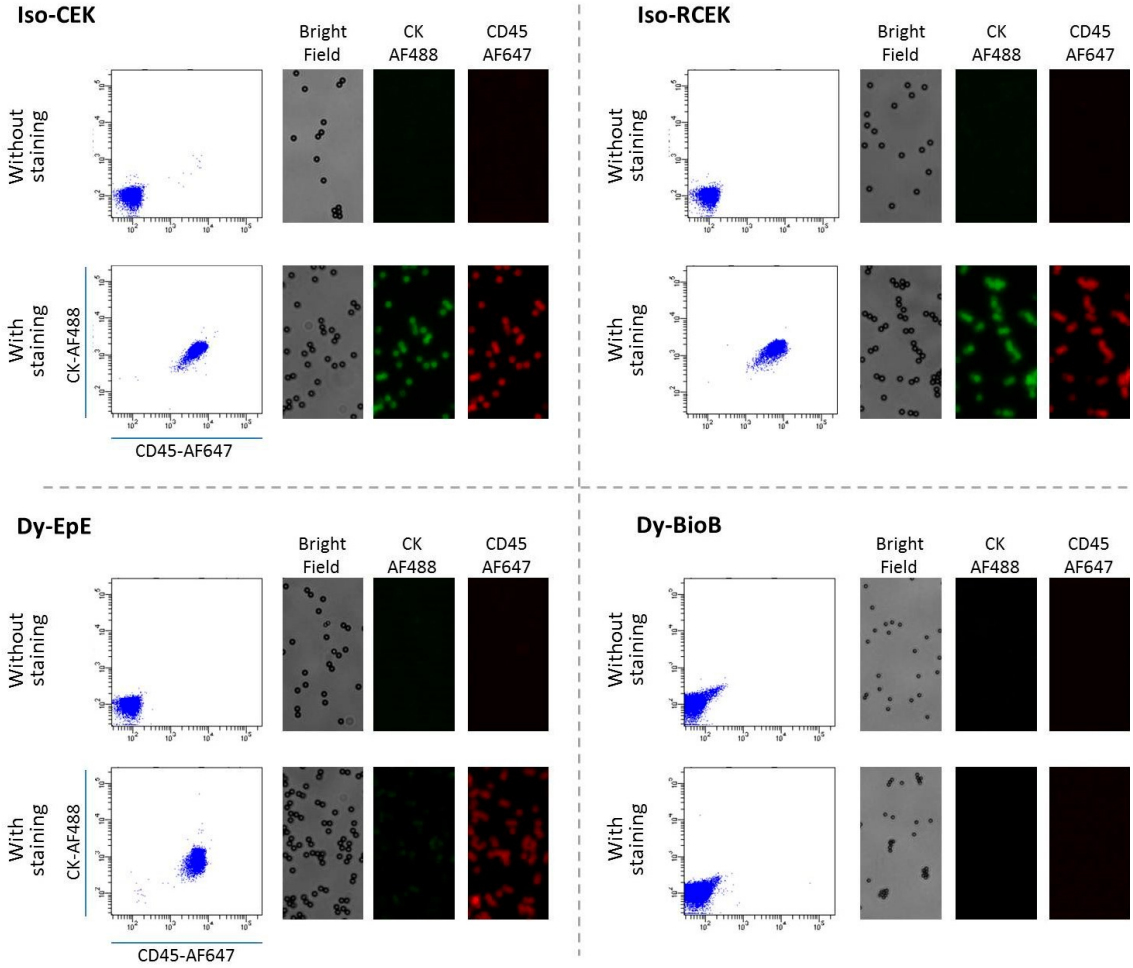

Figure S10. Capturing of staining antibodies by the beads. Flow cytometry and fluorescence microscopy analyses of beads with and without incubation with the complete staining cocktail for clinical samples. Staining was done incubating the beads 40 min in 200 µL of the staining solution and subsequently washing beads once in PBS containing 0.5% BSA and 2 mM EDTA. Flow cytometry analyses were done using a FACSCanto (BD Biosciences, San José, CA, USA). CK-AF488 was analyzed in the FITC channel (Ex 488; Em 530/30) with a voltage of 401 V, and CD45-AF647 in the APC channel (Ex 633; Em 660/20) with a voltage of 456 V. Microscopy analyses were done using an Eclipse E400 (Nikon, Tokyo, Japan) inverted microscope equipped with a 20x objective and a FITC filter (Ex 482/18; Em 520/28) and an APC filter (Ex 640/30; Em 520/28). The exposure time for bright field imaging was 25 ms and for fluorescent imaging 400 ms for both filters.

3 – DISCUSSION

CTCs are very difficult to access and this limited so far our understanding of their biology and their use as biomarkers, respectively. A major challenge hindering CTC accessibility is their extreme rarity and small numbers in standard blood samples. DLA allow sampling liters of blood and several studies have shown now that it increases significantly the number of CTCs that can be obtained from the patients [21,60,65]. However, the high concentration of hematogenous cells in such samples create new challenges for CTC screening and, as consequence, the actual methods can only process a small fraction (~5%) of the complete product. Systems that would allow precise, reliable and cost-effective isolation of CTCs from high volumes of blood and in particular from such high concentrated blood products are still needed. In my project, I investiagted two systems for immunomagnetic enrichment of cells from pancreatic origin spiked in highly concentrated blood products mimicking DLA samples [66]. Immunomagnetic enrichment was chosen because of some advantages compared to other methods based on physical properties of the cells: a) biological: According to the actual knowledge, the phenotype (defined by the expressed proteins) is more relevant for CTC fate than its morphological characteristics (size, deformability, etc..). Therefore, methods that are based on specific cellular markers (e.g EpCAM or MUC-1) might allow us to capture specific populations of CTCs with higher relevance for the clinical course of the disease; b) technical: After capturing, the cells remain in suspension and are more amenable for subsequent isolation (e.g isolation of single cells by micromanipulation or by flow cytometry) for comprehensive molecular characterization.

3.1 – EpCAM and MUC-1 epitopes for enrichment of PDAC cells

In order to define a proper model to test immune-based enrichment of rare pancreatic cells, I started my project by analyzing the expression of different epitopes at the surface of pancreatic cell lines. I used four different cell lines as experimental model in order to better picture the phenotypic heterogeneity of pancreatic tumours.

The EpCAM molecule was chosen because it is largely the most used and validated epitope for the enrichment of CTCs. EpCAM is a type I transmembrane glycoprotein with

a molecular weight of 40 kDa encoded by the GA733-2 gene, which mediate Ca^{+}-independent cell adhesion in epithelial tissues [67]. It was found to be abnormally high expressed in tumour cells and not in blood cells, making it widely studied as an epitope for enrichment of CTCs, namely those with epithelial origin/characteristics [68]. Interestingly, the extracellular domain of EpCAM in tumor cells is easily cleaved by trypsin, a proteinases used for treatment of cell culture cells , leaving only a 6 kDa fragment on the cell surface for recognition [69]. We analyzed EpCAM expression with two different anti-EpCAM antibody clones (Ber-EP4 and VU1D9), both binding to the 6 kDa fragment. Ber-EP4 is a widely used clone in EpCAM-related research for immunostaining [70]. On the other hand, the VU1D9 was chosen because it is the clone used in the CellSearch assays for enrichment of CTCs [71].

In addition to EpCAM, I evaluated two epitopes of MUC-1 (EMA201 and GP1.4) at the surface of the same pancreatic cell lines. MUC-1 is a protein that has been specifically used for pancreatic cancer diagnosis for decades. MUC-1 has a core protein mass of 120-225 kDa and is a member of the mucin family [72]. It is anchored to the cell surface through a transmembrane domain. There is an SEA domain beyond the transmembrane domain that contains a cleavage site for the release of the large extracellular domain. The extracellular domain includes a 20 amino acid variable number tandem repeat (VNTR) domain which are rich in serine, threonine, and proline residues, allowing for heavy o-glycosylation [72]. MUC-1 can bind to p53 and beta-catenin preventing apoptosis and promoting tumour invasion [73], and overexpression of MUC-1 is often observed in tumours. Furthermore, different epitopes of MUC-1-(as CA27.29 and CA15-3) are commonly used tumour markers to detect breast, pancreatic and colorectal cancers [74]. Interestingly, a previous study suggested that combination of anti-EpCAM and anti-MUC-1 antibodies provides more efficient enrichment of Capan-1 cell line cells than each antibody alone [42]. Further, CTC count and phenotype analysis on 50 pancreatic tumor patients with CellSearch system suggest that patients with MUC1-positive CTCs had shorter survival than negative patients suggesting that MUC-1 positivity might identify a sub-set of CTCs particularly relevant for the disease outcome [46].

Table 1 Expression of epitopes on pancreatic cancer cell lines

	EpCAM - Ber-EP4	EpCAM - VU1D9	MUC-1 - EMA201	MUC-1 - GP1.4
Capan-1	23123	203132	367242	391213
Capan-2	42132	321342	388721	542918
Mia-Paca-2	231	432	4213	2312
Hup-T4	123241	452134	12364	19582

The four cell lines differed substantially regarding the investigated epitopes levels (Table 1 and Manuscript's Figure 1). This seems to reflect the heterogeneous nature of pancreatic cancers namely the reported heterogeneous expression patterns of EpCAM in these tumours [75]. Very interestingly, in the three EpCAM positive lines, the number of EpCAM epitopes detected with VU1D9 was much higher than that with Ber-ep4, suggesting that VU1D9 could lead to higher recovery rates.

More notably, the number of MUC-1 epitopes on the cell surface of the Capan-1 and Capan-2 cells was almost 1.5 times higher than EpCAM indicating that the MUC-1 epitope can be efficiently recognised by the respective antibody, and suggesting that this epitope might be even superior for enrichment. Immunostaining in cultured cells confirmed the results found by flow cytometry (Manuscript's Figure 1).

Despite that, when we performed enrichment experiments, the Ber-EP4 clone provided a better recovery rate than the VU1D9 clone and in general recoveries with the MUC-1 antibodies were unsatisfactory lower than with any of the anti-EpCAM antibodies (Manuscript's Figure 1 and 3). These results suggest that, under the experimental conditions and models used, the number of epitopes expressed on the cell surface is not the only factor determining cell recovery with the immunomagnetic particles. Beyond the number of epitopes, there are other factors that could affect the efficiency of CTC collection by immunomagnetic particles: the affinity between antibody and the surface marker, speed of on-rate (the time required for antibody to bind to antigen) and off-rate (duration of antibody-antigen binding), the features of beads and the type of binding between beads and antibodies, and the shear stress resulting from the mixing movement [76]. The strength of antibody binding to epitope can differ between antibodies [77]. Eventually a particularly stronger binding of the Ber-EP4 to its epitope can be the reason for the highest recovery obtained with this antibody despite its lower number of epitopes. In addition, in our experiments, I observed that some of the collected CTCs had very few or even only one magnetic bead attached to their surface, suggesting low off-rate, a fact that should also not be underestimated in CTC enrichment. For example, even

if the antibody and the ligand have a high affinity, their binding may break due to a prolonged incubation time and enrichment steps.

These enrichment experiments were performed spiking cells in 100x10^6 WBCs present in 1mL simulating average DLA samples [21], and therefore these samples were called mimicked DLA samples [21]. DLA samples are limited and the use of the mimicked samples allowed me to expand the number of experiments. Moreover, due to existing differences between patients, DLA products can vary significantly in their cellular content and this can have an impact on the experimental results. Therefore, the use of mimicked DLAs, instead of real DLA samples, allowed standardize experimental conditions over the time of the project.

3.2 –IsoFlux system in DLA mimic samples

The Isoflux is a system capable of capturing magnetic particles circulating in a microchannel under controlled flow conditions. It was developed specifically for enrichment of CTCs using proprietary magnetic beads coupled to EpCAM antibodies. The producer commercialises also magnetic beads for self-conjugation providing the opportunity to test different epitopes for enrichment. Furthermore, before each run in the instrument, the sample needs to be pre-mixed with the magnetic beads, and as this pre-mixing is done manually (and outside of the instrument), several types of beads and different mount of beads can be used. As result, numerous conditions can be tested for enrichment in the system.

The beads available from Fluxion, in particular the beads from the IsoFlux Cell Enrichment Kit (Iso-CEK), which were pre-conjugated with EpCAM antibody, provided by far the highest recoveries in the system (Manuscript's Figure1B). The recovery of Tup-T4, Capan-1 and MIA-PACA-2 cells in the system correlated positively with the previously measured expression of the EpCAM epitope. Beyond the tests done with original beads from the IsoFlux producer, Fluxion (Table 1 and Figure 3 of manuscript), I perfomed several tests with different beads from other providers however the recovery rates were too low and these beads were abandoned (Figure 1).

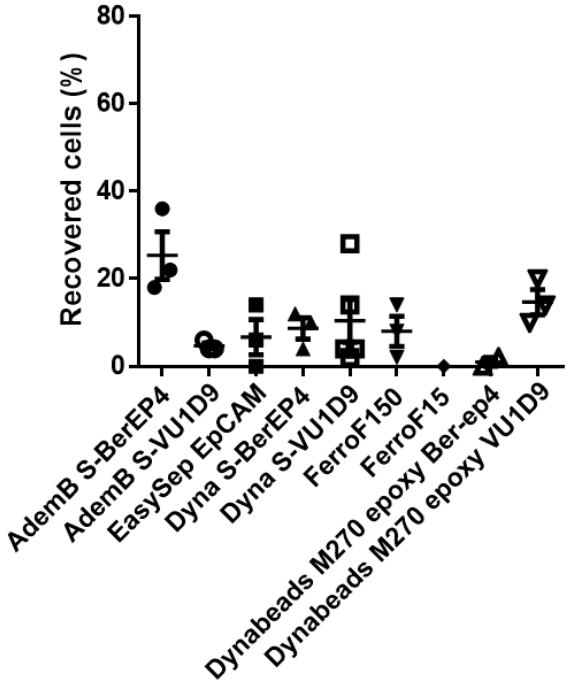

Figure 1 – Recovery of Capan-1 cells spiked in mimicked-DLA samples using different beads conjugated with anti-EpCAM antibody in the IsoFlux system; each bead was tested at least three times (AdemB=Adem beads, EasySep=EasySep beads, Dyna=Dyan cell selection kit beads, Ferro F= Ferro Fluid from the CellSearch system, 15 means 15 µl and 150 means 150 µl per sample).

In the instrument, the flow conditions are pre-defined and the system does not allow to test different flows. The conditions were designed for analysis of standard blood samples and processing highly concentrated mimicked DLA sample seem to interfere with the instrument's flow conditions as I noticed longer running times (45 min for a standard blood sample compared to over 1 hour for mimicked DLA products), and often clogging of the microchannel. Moreover, I often observed the presence of beads in the waste container indicating less efficient capturing of the beads and suggesting that the high concentration of cells in the samples can hinder the effect of the magnetic field pulling the beads. In this aspect, I noted that the Iso-CEK beads also led to less clogging of the microchannel and process failure, which may be due to differences in bead concentration. The experience collected with the system, strongly suggested me that adjusting the flow rates could contribute to reduce the frequency of technical problems affecting the runs and could increase the efficiency of enrichment in such highly concentrated blood samples. However, this is not possible with the actual version of the instrument.

3.3 –KingFisher system in DLA mimic samples

Using the same models to assess the performance of the IsoFlux system, I evaluated the KingFisher system with different types of beads. In the initial experiments, and using one same running protocol designed by me for this system, I could recover spiked cells with most of beads tested although the recovery rates with the Dy-EpE and Dy-BioB beads were highest (Manuscript's Figure 3A). Due to the different properties of the different magnetic beads tested, eventually improved recoveries with the other beads could be achieved upon adapting the running protocol (e.g longer/shorter incubation times, more/less mixing). However, optimization of a protocol specific for each bead type would not be practicable within the time of my project. However, to gain more insights in the conditions determining recovery in the system, I tested three different bead concentrations. The underlying hypothesis was that higher bead concentrations lead to an increased binding surface thereby improving the recovery of spiked cancer cells. I calculated the amount of beads based on the total surface area that they would provide for contact with the cells and allowing to normalize the data for better comparison of the cell recoveries of the beads. Generally, the results were as expected: the higher the number of beads, the higher was the recovery (Manuscript's Figure 3). However, the difference in recovery was not linear between the three tested bead concentrations and, for some cases, the recovery with the medium bead concentration was even higher compared to the highest concentration suggesting that a saturation was reached in the assays. A positive aspect of this was a better identification of tumor cells at medium concentration, since large numbers of beads can create difficulties to identify the target cells. I cannot exclude that some recovered cells remained undetected even upon uniform distribution of the recovered fraction onto the glass slide, and automatic scanning under microscopy (Manuscript's Figure 2).

Moreover, recoveries of CAPAN-1 and Hup-T4 cells with the KingFisher system were in-line or even superior compared to the those obtained with the CellSearch system (Manuscript's Figure S4) and I could also enrich cells from other tumour entities as SK-BR-3 breast cancer cells and HCT116 and SW620 colorectal cancer cells (Manuscript's Figure S7).

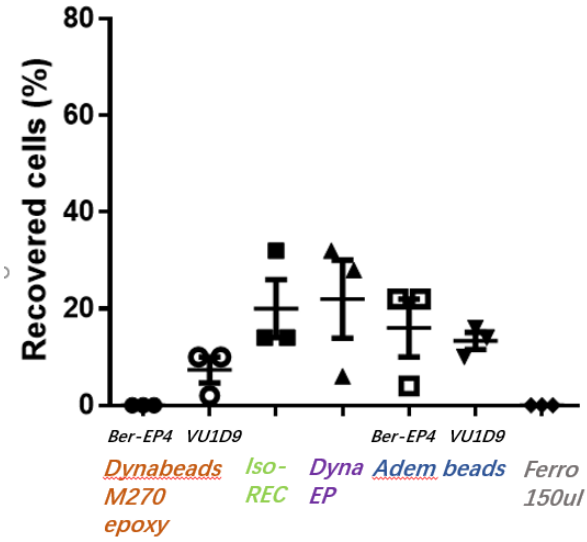

Figure 2 – Different beads conjugated with anti-EpCAM antibodies used in the KingFisher system protocol described above. Each bead was tested at least three times. Dyna Ep= Dyna epithelial enrich kit beads; Ferro Fluid from the CellSearch system is 150 µl per sample; Dynabeads and Adem beads were tested with two anit-EpCAM antibody clones (Ber-EP4 and VU1D9).

Globally, these results show that the KingFisher system has the potential to effectively enrich tumour cells in highly concentrated blood products such as mimicked-DLA samples.

Importantly, for these initial experiments, I used pre-labelled cells which do not require staining after the enrichment and therefore do not completely represent the situation with patient-derived samples. With clinical samples, staining and identification are key parts of the whole detection process and I designed a new protocol combining the previously tested enrichment steps with additional immunostaining performed automatically in the system (WuDuo1S).

Notably, IsoFlux does not have a special device for the staining step, and all staining steps are processed completely manually. The possibility to automate the staining steps in the KingFisher system decreases substantially human intervention and the associated operator-derived errors. The staining protocol used here was based on the CellSearch protocol which uses cytokeratin and nuclear dye as positive markers and the CD45-lymphocyte epitope as an exclusive marker. Upon introduction of additional staining (and necessary washing) steps in the protocol, the recovery rate decreased by approximately 20% (Manuscript's Figure 5). Possible reasons for the decreased recovery might include, heterogeneous staining in the cells that obstruct their subsequent identification as well as disconnection of cells from the beads during the additional pipetting steps using deep-

well plates. To confirm these potential confounding factors, further tests would be necessary.

Considering the high expression of MUC-1 detected at the surface of the investigated cell lines, I tested this epitope for enrichment. I tested MUC-1 antibody-conjugated beads alone and mixed with EpCAM-conjugated beads. In addition, for the KingFisher system I could design a protocol to enrich cells from one same sample sequentially with different beads (WuDuo2) to isolate populations of cells differing in their epitope expression.

Unexpectedly, the recovery rates in both systems with MUC-1 antibody-conjugated beads in both the EMA201 and GP1.4 clones were far lower than those with EpCAM antibody-conjugated beads, although the MUC-1 epitope was expressed at much higher levels than in CAPAN-1 cells. Surprisingly, the combined recovery obtained with EpCAM and MUC-1 beads was identical to the recovery obtained with EpCAM beads alone (Manuscript's Figure 4). The lack of extra gain in total recovery could be a consequence of additional cell losses cause by the additional steps introduced in the protocol for sequential enrichment.

Finally, as the concentration of MNCs is very high in DLA samples which could negatively impact the enrichment of CTCs, I adapted a protocol to perform a MNC negative selection (depletion) before tumour cell positive selection (enrichment). I could observe indeed a reduction of the background cells upon depletion; however, the recovery rate of the spiked cells did not improve (Manuscript's Figure S9) suggesting that the number of background cells in the assay was not a major limitation for enrichment of the rare tumour cells.

3.4 – Final conclusions and perspectives

Collectively, my results show that enrichment of the spiked pancreatic cells is possible with both systems tested, but the efficiency of the KingFisher system was superior [66]. Moreover, the KingFisher system is easy to program and adapt protocols for the specific needs of the assay (e.g type of samples, type of beads). It gives users many options and the opportunity to integrate additional steps, such as immunostaining, negative and positive selection, and step-wise selection using multiple beads. It could also perform automated DNA purification downstream to enrichment for molecular analyses

of the bulk enriched fraction (not tested in the current project). This level of flexibility is particularly interesting considering the early stage of CTC research, where much is still unknown on the phenotype and molecular properties of these cells. In the initial phase of the project, the high flexibility of the system and the absence of protocols designed for CTCs created some difficulties to find suitable experimental protocols for our samples. However, once the protocols were set, they could be reproducibly run in the instrument and the protocols designed can be exported and easily transferred to be run at other locations allowing multi-centre studies or be the basis of further developments.

The positive results obtained motivate future experiments using clinical DLA samples. However, the diversity in cell content and quality that can be observed in DLA products will certainly impose new challenges. Additional challenges might come from the difficulty to identify the cells among the excess of magnetic beads after enrichment, a fact that applies also to Isoflux and any other system working with large magnetic beads. In the present project, the identification of the enriched cell line cells was facilitated by their pre-staining and by their known strong expression of cytokeratins, the positive marker used for identification. However, in clinical samples, the expression of cytokeratins in CTCs is heterogeneous and the identification of cells that might require more sophisticated microscopy or methods for image recognition. Overcoming this last challenge would be critical to use the system for systematic analysis (e.g. in clinical studies).

In summary, our results demonstrate the good performance of the KingFisher system to enrich rare cells in the high concentrated blood samples and highlight several characteristics of the system that makes it attractive for both for research and clinical purposes.

4 – References

1. Wang, H.; Naghavi, M.; Allen, C.; Barber, R.M.; Bhutta, Z.A.; Carter, A.; Casey, D.C.; Charlson, F.J.; Chen, A.Z.; Coates, M.M.; et al. Global, regional, and national life expectancy, all-cause mortality, and cause-specific mortality for 249 causes of death, 1980–2015: a systematic analysis for the Global Burden of Disease Study 2015. *The Lancet* **2016**, *388*, 1459–1544, doi:10.1016/S0140-6736(16)31012-1.
2. Kulemann, B.; Rösch, S.; Seifert, S.; Timme, S.; Bronsert, P.; Seifert, G.; Martini, V.; Kuvendjiska, J.; Glatz, T.; Hussung, S.; et al. Pancreatic cancer: Circulating Tumor Cells and Primary Tumors show Heterogeneous KRAS Mutations. *Sci Rep* **2017**, *7*, 4510, doi:10.1038/s41598-017-04601-z.
3. Neoptolemos, J.P.; Palmer, D.H.; Ghaneh, P.; Psarelli, E.E.; Valle, J.W.; Halloran, C.M.; Faluyi, O.; O'Reilly, D.A.; Cunningham, D.; Wadsley, J.; et al. Comparison of adjuvant gemcitabine and capecitabine with gemcitabine monotherapy in patients with resected pancreatic cancer (ESPAC-4): a multicentre, open-label, randomised, phase 3 trial. *The Lancet* **2017**, *389*, 1011–1024, doi:10.1016/S0140-6736(16)32409-6.
4. Toyama, Y.; Hotta, M.; Motoi, F.; Takanami, K.; Minamimoto, R.; Takase, K. Prognostic value of FDG-PET radiomics with machine learning in pancreatic cancer. *Sci Rep* **2020**, *10*, 17024, doi:10.1038/s41598-020-73237-3.
5. Hauch, S.; Zimmermann, S.; Lankiewicz, S.; Zieglschmid, V.; Böcher, O.; Albert, W.H. The clinical significance of circulating tumour cells in breast cancer and colorectal cancer patients. *Anticancer Res.* **2007**, *27*, 1337–1341.
6. Heerboth, S.; Housman, G.; Leary, M.; Longacre, M.; Byler, S.; Lapinska, K.; Willbanks, A.; Sarkar, S. EMT and tumor metastasis. *Clin. Transl. Med.* **2015**, *4*, 6, doi:10.1186/s40169-015-0048-3.
7. Wang, H.; Stoecklein, N.H.; Lin, P.P.; Gires, O. Circulating and disseminated tumor cells: diagnostic tools and therapeutic targets in motion. *Oncotarget* **2017**, *8*, 1884–1912, doi:10.18632/oncotarget.12242.
8. Pantel, K.; Speicher, M.R. The biology of circulating tumor cells. *Oncogene* **2016**, *35*, 1216–1224, doi:10.1038/onc.2015.192.
9. Cristofanilli, M.; Hayes, D.F.; Budd, G.T.; Ellis, M.J.; Stopeck, A.; Reuben, J.M.; Doyle, G.V.; Matera, J.; Allard, W.J.; Miller, M.C.; et al. Circulating tumor cells: a

novel prognostic factor for newly diagnosed metastatic breast cancer. *J. Clin. Oncol.* **2005**, *23*, 1420–1430, doi:10.1200/JCO.2005.08.140.

10. Effenberger, K.E.; Schroeder, C.; Hanssen, A.; Wolter, S.; Eulenburg, C.; Tachezy, M.; Gebauer, F.; Izbicki, J.R.; Pantel, K.; Bockhorn, M. Improved Risk Stratification by Circulating Tumor Cell Counts in Pancreatic Cancer. *Clin. Cancer Res.* **2018**, *24*, 2844–2850, doi:10.1158/1078-0432.CCR-18-0120.
11. Hugenschmidt, H.; Labori, K.J.; Brunborg, C.; Verbeke, C.S.; Seeberg, L.T.; Schirmer, C.B.; Renolen, A.; Borgen, E.F.; Naume, B.; Wiedswang, G. Circulating Tumor Cells are an Independent Predictor of Shorter Survival in Patients Undergoing Resection for Pancreatic and Periampullary Adenocarcinoma. *Annals of Surgery* **2020**, *271*, 549–558, doi:10.1097/SLA.0000000000003035.
12. White, M.G.; Lee, A.; Vicente, D.; Hall, C.; Kim, M.P.; Katz, M.H.G.; Lee, J.E.; Ikoma, N.; Lucci, A.; Tzeng, C.-W.D. Measurement of Portal Vein Blood Circulating Tumor Cells is Safe and May Correlate With Outcomes in Resected Pancreatic Ductal Adenocarcinoma. *Ann Surg Oncol* **2021**, *28*, 4615–4622, doi:10.1245/s10434-020-09518-y.
13. Okubo, K.; Uenosono, Y.; Arigami, T.; Mataki, Y.; Matsushita, D.; Yanagita, S.; Kurahara, H.; Sakoda, M.; Kijima, Y.; Maemura, K.; et al. Clinical impact of circulating tumor cells and therapy response in pancreatic cancer. *Eur. J. Surg. Oncol.* **2017**, *43*, 1050–1055, doi:10.1016/j.ejso.2017.01.241.
14. Miller, M.C.; Doyle, G.V.; Terstappen, L.W.M.M. Significance of Circulating Tumor Cells Detected by the CellSearch System in Patients with Metastatic Breast Colorectal and Prostate Cancer. *J. Oncol.* **2010**, *2010*, 617421, doi:10.1155/2010/617421.
15. Riethdorf, S.; Fritsche, H.; Müller, V.; Rau, T.; Schindlbeck, C.; Rack, B.; Janni, W.; Coith, C.; Beck, K.; Jänicke, F.; et al. Detection of circulating tumor cells in peripheral blood of patients with metastatic breast cancer: a validation study of the CellSearch system. *Clin. Cancer Res.* **2007**, *13*, 920–928, doi:10.1158/1078-0432.CCR-06-1695.
16. Alix-Panabières, C.; Pantel, K. Challenges in circulating tumour cell research. *Nat. Rev. Cancer* **2014**, *14*, 623–631, doi:10.1038/nrc3820.

17. Krebs, M.G.; Metcalf, R.L.; Carter, L.; Brady, G.; Blackhall, F.H.; Dive, C. Molecular analysis of circulating tumour cells-biology and biomarkers. *Nat. Rev. Clin. Oncol.* **2014**, *11*, 129–144, doi:10.1038/nrclinonc.2013.253.
18. Koch, C.; Joosse, S.A.; Schneegans, S.; Wilken, O.J.W.; Janning, M.; Loreth, D.; Müller, V.; Prieske, K.; Banys-Paluchowski, M.; Horst, L.J.; et al. Pre-Analytical and Analytical Variables of Label-Independent Enrichment and Automated Detection of Circulating Tumor Cells in Cancer Patients. *Cancers (Basel)* **2020**, *12*, doi:10.3390/cancers12020442.
19. Plouffe, B.D.; Murthy, S.K.; Lewis, L.H. Fundamentals and application of magnetic particles in cell isolation and enrichment: a review. *Rep. Prog. Phys.* **2015**, *78*, 16601, doi:10.1088/0034-4885/78/1/016601.
20. Lee, A.-W.; Lin, F.-X.; Wei, P.-L.; Jian-Wei, G.; Chen, J.-K. Binary-blend fibber-based capture assay of circulating tumor cells for clinical diagnosis of colorectal cancer. *J. Nanobiotechnology* **2018**, *16*, 4, doi:10.1186/s12951-017-0330-1.
21. Guglielmi, R.; Lai, Z.; Raba, K.; van Dalum, G.; Wu, J.; Behrens, B.; Bhagat, A.A.S.; Knoefel, W.T.; Neves, R.P.L.; Stoecklein, N.H. Technical validation of a new microfluidic device for enrichment of CTCs from large volumes of blood by using buffy coats to mimic diagnostic leukapheresis products. *Sci Rep* **2020**, *10*, 20312, doi:10.1038/s41598-020-77227-3.
22. Di Trapani, M.; Manaresi, N.; Medoro, G. DEPArray™ system: An automatic image-based sorter for isolation of pure circulating tumor cells. *Cytometry A.* **2018**, *93*, 1260–1266, doi:10.1002/cyto.a.23687.
23. Gabriel, M.T.; Calleja, L.R.; Chalopin, A.; Ory, B.; Heymann, D. Circulating Tumor Cells: A Review of Non-EpCAM-Based Approaches for Cell Enrichment and Isolation. *Clin. Chem.* **2016**, *62*, 571–581, doi:10.1373/clinchem.2015.249706.
24. Bidard, F.C.; Huguet, F.; Louvet, C.; Mineur, L.; Bouché, O.; Chibaudel, B.; Artru, P.; Desseigne, F.; Bachet, J.B.; Mathiot, C.; et al. Circulating tumor cells in locally advanced pancreatic adenocarcinoma: the ancillary CirCe 07 study to the LAP 07 trial. *Ann. Oncol.* **2013**, *24*, 2057–2061, doi:10.1093/annonc/mdt176.
25. Mandair, D.; Khan, M.S.; Lopes, A.; Furtado O'Mahony, L.; Ensell, L.; Lowe, H.; Hartley, J.A.; Toumpanakis, C.; Caplin, M.; Meyer, T. Prognostic Threshold for Circulating Tumor Cells in Patients With Pancreatic and Midgut Neuroendocrine

Tumors. *The Journal of Clinical Endocrinology & Metabolism* **2021**, *106*, 872–882, doi:10.1210/clinem/dgaa822.

26. Kurihara, T.; Itoi, T.; Sofuni, A.; Itokawa, F.; Tsuchiya, T.; Tsuji, S.; Ishii, K.; Ikeuchi, N.; Tsuchida, A.; Kasuya, K.; et al. Detection of circulating tumor cells in patients with pancreatic cancer: a preliminary result. *J. Hepatobiliary. Pancreat. Surg.* **2008**, *15*, 189–195, doi:10.1007/s00534-007-1250-5.
27. Wei, T.; Zhang, X.; Zhang, Q.; Yang, J.; Chen, Q.; Wang, J.; Li, X.; Chen, J.; Ma, T.; Li, G.; et al. Vimentin-positive circulating tumor cells as a biomarker for diagnosis and treatment monitoring in patients with pancreatic cancer. *Cancer Letters* **2019**, *452*, 237–243, doi:10.1016/j.canlet.2019.03.009.
28. *Microsieves for the detection of circulating tumor cells in leukapheresis product in non-small cell lung cancer patients*, 2020.
29. Khoja, L.; Backen, A.; Sloane, R.; Menasce, L.; Ryder, D.; Krebs, M.; Board, R.; Clack, G.; Hughes, A.; Blackhall, F.; et al. A pilot study to explore circulating tumour cells in pancreatic cancer as a novel biomarker. *Br. J. Cancer* **2012**, *106*, 508–516, doi:10.1038/bjc.2011.545.
30. Earl, J.; Garcia-Nieto, S.; Martinez-Avila, J.C.; Montans, J.; Sanjuanbenito, A.; Rodríguez-Garrote, M.; Lisa, E.; Mendía, E.; Lobo, E.; Malats, N.; et al. Circulating tumor cells (Ctc) and kras mutant circulating free Dna (cfdna) detection in peripheral blood as biomarkers in patients diagnosed with exocrine pancreatic cancer. *BMC Cancer* **2015**, *15*, 797, doi:10.1186/s12885-015-1779-7.
31. Gemenetzis, G.; Groot, V.P.; Yu, J.; Ding, D.; Teinor, J.A.; Javed, A.A.; Wood, L.D.; Burkhart, R.A.; Cameron, J.L.; Makary, M.A.; et al. Circulating Tumor Cells Dynamics in Pancreatic Adenocarcinoma Correlate With Disease Status: Results of the Prospective CLUSTER Study. *Annals of Surgery* **2018**, *268*, 408–420, doi:10.1097/SLA.0000000000002925.
32. Kim, H.; Heo, C.M.; Oh, J.; Lee, E.M.; Park, J.; Lee, S.-H.; Lee, K.H.; Lee, K.T.; Lee, J.K.; Cho, Y.-K.; et al. *Clinical Significance of Circulating Tumor Cells in Unresectable Pancreatic Ductal Adenocarcinomas*, 2021.
33. Song, B.G.; Kwon, W.; Kim, H.; Lee, E.M.; Han, Y.M.; Kim, H.; Byun, Y.; Lee, K.B.; Lee, K.H.; Lee, K.T.; et al. Detection of Circulating Tumor Cells in Resectable Pancreatic Ductal Adenocarcinoma: A Prospective Evaluation as a

Prognostic Marker. *Front. Oncol.* **2020**, *10*, 616440, doi:10.3389/fonc.2020.616440.

34. Akita, H.; Nagano, H.; Takeda, Y.; Eguchi, H.; Wada, H.; Kobayashi, S.; Marubashi, S.; Tanemura, M.; Takahashi, H.; Ohigashi, H.; et al. Ep-CAM is a significant prognostic factor in pancreatic cancer patients by suppressing cell activity. *Oncogene* **2011**, *30*, 3468–3476, doi:10.1038/onc.2011.59.
35. Fong, D.; Steurer, M.; Obrist, P.; Barbieri, V.; Margreiter, R.; Amberger, A.; Laimer, K.; Gastl, G.; Tzankov, A.; Spizzo, G. Ep-CAM expression in pancreatic and ampullary carcinomas: frequency and prognostic relevance. *J. Clin. Pathol.* **2008**, *61*, 31–35, doi:10.1136/jcp.2006.037333.
36. Raimondi, C.; Gradilone, A.; Naso, G.; Vincenzi, B.; Petracca, A.; Nicolazzo, C.; Palazzo, A.; Saltarelli, R.; Spremberg, F.; Cortesi, E.; et al. Epithelial-mesenchymal transition and stemness features in circulating tumor cells from breast cancer patients. *Breast Cancer Res. Treat.* **2011**, *130*, 449–455, doi:10.1007/s10549-011-1373-x.
37. Wu, S.; Liu, S.; Liu, Z.; Huang, J.; Pu, X.; Li, J.; Yang, D.; Deng, H.; Yang, N.; Xu, J. Classification of circulating tumor cells by epithelial-mesenchymal transition markers. *PLoS ONE* **2015**, *10*, e0123976, doi:10.1371/journal.pone.0123976.
38. Yu, M.; Bardia, A.; Wittner, B.S.; Stott, S.L.; Smas, M.E.; Ting, D.T.; Isakoff, S.J.; Ciciliano, J.C.; Wells, M.N.; Shah, A.M.; et al. Circulating breast tumor cells exhibit dynamic changes in epithelial and mesenchymal composition. *Science* **2013**, *339*, 580–584, doi:10.1126/science.1228522.
39. Gorges, T.M.; Tinhofer, I.; Drosch, M.; Röse, L.; Zollner, T.M.; Krahn, T.; Ahsen, O. von. Circulating tumour cells escape from EpCAM-based detection due to epithelial-to-mesenchymal transition. *BMC Cancer* **2012**, *12*, 178, doi:10.1186/1471-2407-12-178.
40. Li, Y.; Cozzi, P.J. MUC1 is a promising therapeutic target for prostate cancer therapy. *Curr. Cancer Drug Targets* **2007**, *7*, 259–271, doi:10.2174/156800907780618338.
41. Gold, D.V.; Cardillo, T.; Goldenberg, D.M.; Sharkey, R.M. Localization of pancreatic cancer with radiolabeled monoclonal antibody PAM4. *Crit. Rev. Oncol. Hematol.* **2001**, *39*, 147–154, doi:10.1016/s1040-8428(01)00114-7.

42. Thege, F.I.; Lannin, T.B.; Saha, T.N.; Tsai, S.; Kochman, M.L.; Hollingsworth, M.A.; Rhim, A.D.; Kirby, B.J. Microfluidic immunocapture of circulating pancreatic cells using parallel EpCAM and MUC1 capture: characterization, optimization and downstream analysis. *Lab Chip* **2014**, *14*, 1775–1784, doi:10.1039/c4lc00041b.
43. Chebouti, I.; Kasimir-Bauer, S.; Buderath, P.; Wimberger, P.; Hauch, S.; Kimmig, R.; Kuhlmann, J.D. EMT-like circulating tumor cells in ovarian cancer patients are enriched by platinum-based chemotherapy. *Oncotarget* **2017**, *8*, 48820–48831, doi:10.18632/oncotarget.16179.
44. Blassl, C.; Kuhlmann, J.D.; Webers, A.; Wimberger, P.; Fehm, T.; Neubauer, H. Gene expression profiling of single circulating tumor cells in ovarian cancer - Establishment of a multi-marker gene panel. *Mol. Oncol.* **2016**, *10*, 1030–1042, doi:10.1016/j.molonc.2016.04.002.
45. Aktas, B.; Kasimir-Bauer, S.; Müller, V.; Janni, W.; Fehm, T.; Wallwiener, D.; Pantel, K.; Tewes, M. Comparison of the HER2, estrogen and progesterone receptor expression profile of primary tumor, metastases and circulating tumor cells in metastatic breast cancer patients. *BMC Cancer* **2016**, *16*, 522, doi:10.1186/s12885-016-2587-4.
46. Dotan, E.; Alpaugh, R.K.; Ruth, K.; Negin, B.P.; Denlinger, C.S.; Hall, M.J.; Astsaturov, I.; McAleer, C.; Fittipaldi, P.; Thrash-Bingham, C.; et al. Prognostic Significance of MUC-1 in Circulating Tumor Cells in Patients With Metastatic Pancreatic Adenocarcinoma. *Pancreas* **2016**, *45*, 1131–1135, doi:10.1097/MPA.0000000000000619.
47. Brychta, N.; Drosch, M.; Driemel, C.; Fischer, J.C.; Neves, R.P.; Esposito, I.; Knoefel, W.; Möhlendick, B.; Hille, C.; Stresemann, A.; et al. Isolation of circulating tumor cells from pancreatic cancer by automated filtration. *Oncotarget* **2017**, *8*, 86143–86156, doi:10.18632/oncotarget.21026.
48. Harouaka, R.A.; Nisic, M.; Zheng, S.-Y. Circulating tumor cell enrichment based on physical properties. *J. Lab. Autom.* **2013**, *18*, 455–468, doi:10.1177/2211068213494391.
49. Harb, W.; Fan, A.; Tran, T.; Danila, D.C.; Keys, D.; Schwartz, M.; Ionescu-Zanetti, C. Mutational Analysis of Circulating Tumor Cells Using a Novel

Microfluidic Collection Device and qPCR Assay. *Transl. Oncol.* **2013**, *6*, 528–538, doi:10.1593/tlo.13367.

50. Xu, L.; Mao, X.; Imrali, A.; Syed, F.; Mutsvangwa, K.; Berney, D.; Cathcart, P.; Hines, J.; Shamash, J.; Lu, Y.-J. Optimization and Evaluation of a Novel Size Based Circulating Tumor Cell Isolation System. *PLoS ONE* **2015**, *10*, e0138032, doi:10.1371/journal.pone.0138032.
51. Sánchez-Lorencio, M.I.; Ramirez, P.; Saenz, L.; Martínez Sánchez, M.V.; La Orden, V. de; Mediero-Valeros, B.; Veganzones-De-Castro, S.; Baroja-Mazo, A.; Revilla Nuin, B.; Gonzalez, M.R.; et al. Comparison of Two Types of Liquid Biopsies in Patients With Hepatocellular Carcinoma Awaiting Orthotopic Liver Transplantation. *Transplant. Proc.* **2015**, *47*, 2639–2642, doi:10.1016/j.transproceed.2015.10.003.
52. Alva, A.; Friedlander, T.; Clark, M.; Huebner, T.; Daignault, S.; Hussain, M.; Lee, C.; Hafez, K.; Hollenbeck, B.; Weizer, A.; et al. Circulating Tumor Cells as Potential Biomarkers in Bladder Cancer. *J. Urol.* **2015**, *194*, 790–798, doi:10.1016/j.juro.2015.02.2951.
53. Cabezas-Camarero, S.; La Orden-García, V. de; Veganzones-de-Castro, S.; Mediero-Valeros, B.; Fuentes-Ferrer, M.E.; Sánchez Ruiz, A.C.; Provencio, M.; Aranda, E.; Sastre Valera, J.; Diaz-Rubio, E. Performance of two immunoafinity-based methods for CTC detection and molecular characterization in advanced colorectal cancer. *JCO* **2018**, *36*, e15648-e15648, doi:10.1200/JCO.2018.36.15_suppl.e15648.
54. Cabezas-Camarero, S.; La Orden, V. de; Veganzones-de-Castro, S.; Medievo-Valeros, B.; Fuentes-Ferrer, M.E.; Sánchez-Ruiz, A.; Provencio, M.; Aranda, E.; Sastre, J.; Díaz-Rubio, E. *Comparison of Two EpCAM-Based Methods for CTC Detection and Molecular Characterization in Advanced Colorectal Cancer*, 2016.
55. Agerbæk, M.Ø.; Bang-Christensen, S.R.; Yang, M.-H.; Clausen, T.M.; Pereira, M.A.; Sharma, S.; Ditlev, S.B.; Nielsen, M.A.; Choudhary, S.; Gustavsson, T.; et al. The VAR2CSA malaria protein efficiently retrieves circulating tumor cells in an EpCAM-independent manner. *Nat. Commun.* **2018**, *9*, 3279, doi:10.1038/s41467-018-05793-2.
56. Yang, G.; Erdman, D.E.; Kodani, M.; Kools, J.; Bowen, M.D.; Fields, B.S. Comparison of commercial systems for extraction of nucleic acids from

DNA/RNA respiratory pathogens. *J. Virol. Methods* **2011**, *171*, 195–199, doi:10.1016/j.jviromet.2010.10.024.

57. Arola, H.O.; Tullila, A.; Kiljunen, H.; Campbell, K.; Siitari, H.; Nevanen, T.K. Specific Noncompetitive Immunoassay for HT-2 Mycotoxin Detection. *Anal. Chem.* **2016**, *88*, 2446–2452, doi:10.1021/acs.analchem.5b04591.
58. Stoecklein, N.H.; Fischer, J.C.; Niederacher, D.; Terstappen, L.W.M.M. Challenges for CTC-based liquid biopsies: low CTC frequency and diagnostic leukapheresis as a potential solution. *Expert Rev. Mol. Diagn.* **2016**, *16*, 147–164, doi:10.1586/14737159.2016.1123095.
59. Fischer, J.C.; Niederacher, D.; Topp, S.A.; Honisch, E.; Schumacher, S.; Schmitz, N.; Zacarias Föhrding, L.; Vay, C.; Hoffmann, I.; Kasprowicz, N.S.; et al. Diagnostic leukapheresis enables reliable detection of circulating tumor cells of nonmetastatic cancer patients. *Proc. Natl. Acad. Sci. U. S. A.* **2013**, *110*, 16580–16585, doi:10.1073/pnas.1313594110.
60. Andree, K.C.; Mentink, A.; Zeune, L.L.; Terstappen, L.W.M.M.; Stoecklein, N.H.; Neves, R.P.; Driemel, C.; Lampignano, R.; Yang, L.; Neubauer, H.; et al. Toward a real liquid biopsy in metastatic breast and prostate cancer: Diagnostic LeukApheresis increases CTC yields in a European prospective multicenter study (CTCTrap). *Int. J. Cancer* **2018**, *143*, 2584–2591, doi:10.1002/ijc.31752.
61. Lambros, M.B.; Seed, G.; Sumanasuriya, S.; Gil, V.; Crespo, M.; Fontes, M.; Chandler, R.; Mehra, N.; Fowler, G.; Ebbs, B.; et al. Single-Cell Analyses of Prostate Cancer Liquid Biopsies Acquired by Apheresis. *Clin. Cancer Res.* **2018**, *24*, 5635–5644, doi:10.1158/1078-0432.CCR-18-0862.
62. Fehm, T.N.; Meier-Stiegen, F.; Driemel, C.; Jäger, B.; Reinhardt, F.; Naskou, J.; Franken, A.; Neubauer, H.; Neves, R.P.L.; van Dalum, G.; et al. Diagnostic leukapheresis for CTC analysis in breast cancer patients: CTC frequency, clinical experiences and recommendations for standardized reporting. *Cytometry A* **2018**, *93*, 1213–1219, doi:10.1002/cyto.a.23669.
63. Hahn, G.; Stuhlmüller, B.; Hain, N.; Kalden, J.R.; Pfizenmaier, K.; Burmester, G.R. Modulation of monocyte activation in patients with rheumatoid arthritis by leukapheresis therapy. *J. Clin. Invest.* **1993**, *91*, 862–870, doi:10.1172/JCI116307.
64. Tamminga, M.; Oomens, L.; Hiltermann, T.J.N.; Andree, K.C.; Tibbe, A.; Broekmaat, J.; Schuuring, E.; Terstappen, L.W.M.M.; Groen, H.J.M. Microsieves

for the detection of circulating tumor cells in leukapheresis product in non-small cell lung cancer patients. *Transl. Lung Cancer Res.* **2020**, *9*, 1093–1100, doi:10.21037/tlcr-19-413.

65. Franken, A.; Driemel, C.; Behrens, B.; Meier-Stiegen, F.; Endris, V.; Stenzinger, A.; Niederacher, D.; Fischer, J.C.; Stoecklein, N.H.; Ruckhaeberle, E.; et al. Label-Free Enrichment and Molecular Characterization of Viable Circulating Tumor Cells from Diagnostic Leukapheresis Products. *Clin. Chem.* **2019**, *65*, 549–558, doi:10.1373/clinchem.2018.296814.
66. Wu, J.; Raba, K.; Guglielmi, R.; Behrens, B.; van Dalum, G.; Flügen, G.; Koch, A.; Patel, S.; Knoefel, W.T.; Stoecklein, N.H.; et al. Magnetic-Based Enrichment of Rare Cells from High Concentrated Blood Samples. *Cancers (Basel)* **2020**, *12*, doi:10.3390/cancers12040933.
67. Went, P.T.; Lugli, A.; Meier, S.; Bundi, M.; Mirlacher, M.; Sauter, G.; Dirnhofer, S. Frequent EpCam protein expression in human carcinomas. *Hum. Pathol.* **2004**, *35*, 122–128, doi:10.1016/j.humpath.2003.08.026.
68. Keller, L.; Werner, S.; Pantel, K. Biology and clinical relevance of EpCAM. *Cell Stress* **2019**, *3*, 165–180, doi:10.15698/cst2019.06.188.
69. Chantima, W.; Thepthai, C.; Cheunsuchon, P.; Dharakul, T. EpCAM expression in squamous cell carcinoma of the uterine cervix detected by monoclonal antibody to the membrane-proximal part of EpCAM. *BMC Cancer* **2017**, *17*, 811, doi:10.1186/s12885-017-3798-z.
70. Schehr, J.L.; Schultz, Z.D.; Warrick, J.W.; Guckenberger, D.J.; Pezzi, H.M.; Sperger, J.M.; Heninger, E.; Saeed, A.; Leal, T.; Mattox, K.; et al. High Specificity in Circulating Tumor Cell Identification Is Required for Accurate Evaluation of Programmed Death-Ligand 1. *PLoS ONE* **2016**, *11*, e0159397, doi:10.1371/journal.pone.0159397.
71. Andree, K.C.; van Dalum, G.; Terstappen, L.W.M.M. Challenges in circulating tumor cell detection by the CellSearch system. *Mol. Oncol.* **2016**, *10*, 395–407, doi:10.1016/j.molonc.2015.12.002.
72. Qu, C.F.; Li, Y.; Song, Y.J.; Rizvi, S.M.A.; Raja, C.; Zhang, D.; Samra, J.; Smith, R.; Perkins, A.C.; Apostolidis, C.; et al. MUC1 expression in primary and metastatic pancreatic cancer cells for in vitro treatment by (213)Bi-C595

radioimmunoconjugate. *Br. J. Cancer* **2004**, *91*, 2086–2093, doi:10.1038/sj.bjc.6602232.

73. Wei, X.; Xu, H.; Kufe, D. Human MUC1 oncoprotein regulates p53-responsive gene transcription in the genotoxic stress response. *Cancer Cell* **2005**, *7*, 167–178, doi:10.1016/j.ccr.2005.01.008.
74. Yamamoto, M.; Bharti, A.; Li, Y.; Kufe, D. Interaction of the DF3/MUC1 breast carcinoma-associated antigen and beta-catenin in cell adhesion. *J. Biol. Chem.* **1997**, *272*, 12492–12494, doi:10.1074/jbc.272.19.12492.
75. Gires, O.; Stoecklein, N.H. Dynamic EpCAM expression on circulating and disseminating tumor cells: causes and consequences. *Cell. Mol. Life Sci.* **2014**, *71*, 4393–4402, doi:10.1007/s00018-014-1693-1.
76. Münz, M.; Murr, A.; Kvesic, M.; Rau, D.; Mangold, S.; Pflanz, S.; Lumsden, J.; Volkland, J.; Fagerberg, J.; Riethmüller, G.; et al. Side-by-side analysis of five clinically tested anti-EpCAM monoclonal antibodies. *Cancer Cell Int.* **2010**, *10*, 44, doi:10.1186/1475-2867-10-44.
77. Kuo, S.C.; Lauffenburger, D.A. Relationship between receptor/ligand binding affinity and adhesion strength. *Biophys. J.* **1993**, *65*, 2191–2200, doi:10.1016/S0006-3495(93)81277-3.

ACKNOWLEDGEMENTS

I would like to express my deep sense of thanks and gratitude to my mentor and guide **Univ.-Prof. Dr. med. Nikolas H. Stoecklein**, head of research at Department of General-, Visceral- and Paediatric Surgery at the Heinrich Heine University Düsseldorf. His insight and knowledge into the subject matter steered me through the research.

I am also thankful to **Dr. rer. nat. Rui P. L. Neves**, without him I would not have able to complete this research. And I would like to extend my sincere thanks to **Dr. rer. nat. Bianca Behrens, Christiane Driemel, Maria Wecker, Swetlana Seidschner and all students** for the advice and support in the lab.

At last, I would be remiss in not mentioning **My family**, for their love, support and constant encouragement throughout my research period.